LEARN FASTER, LEARN BETTER!

BOOCs EPFL

Introduction to Astrophysics
Frédéric Courbin

INTRODUCTION TO ASTROPHYSICS

Frédéric Courbin

LEARN FASTER, LEARN BETTER!

BOOCs EPFL

Introduction to Astrophysics
Frédéric Courbin

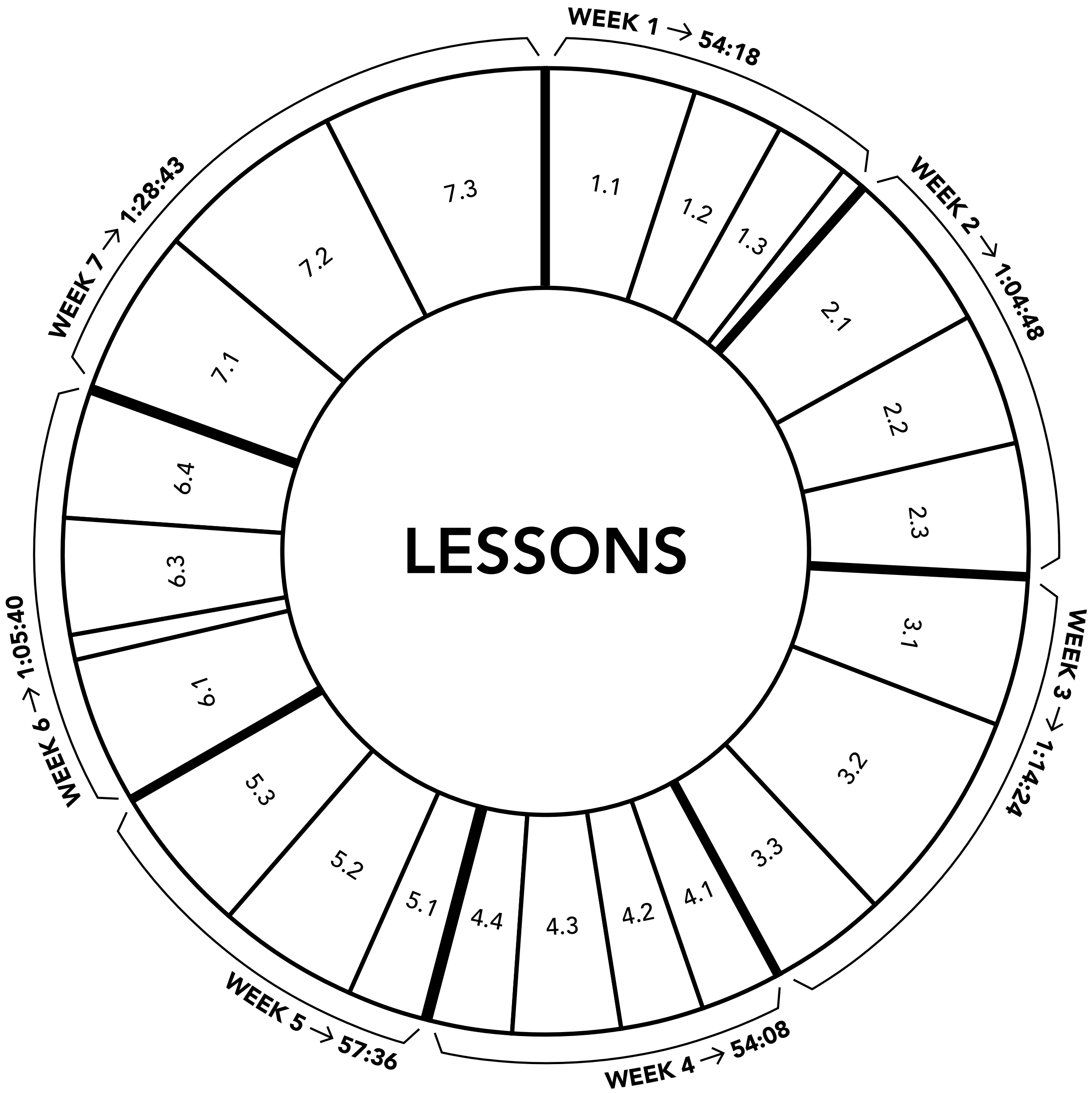

CONTENT

1.1 BRIEF OVERVIEW

In the solar system, we use the distance scale of *astronomical units* (au). One astronomical unit is equal to the distance between the Earth and the Sun, i.e. 149 million kilometres.

$$1\,\text{au} = 149 \cdot 10^{6}\ \text{km}$$

If we need to reference larger distances, we will often use *light-years* (ly). One light-year is equal to the distance travelled by light in one year, at a speed of 300,000 km/s.

$$1\ \text{ly} = 9.44 \cdot 10^{12}\ \text{km}$$

However, more commonly, we will use *parsecs* or pc.

$$1\ \text{pc} = 3.26\,\text{ly} = 3.085 \cdot 10^{13}\ \text{km}$$

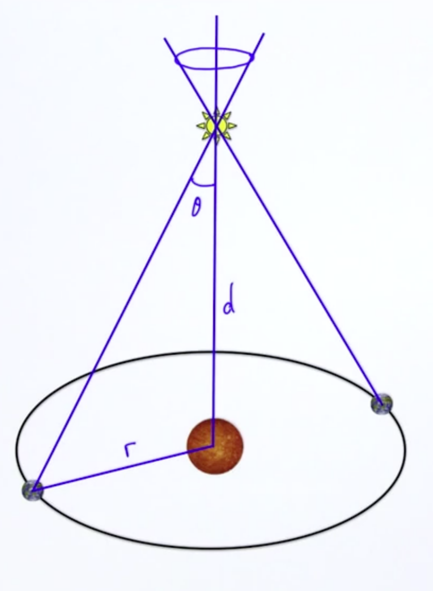

FIGURE 1

3:28 23:00

Parallax.

PARALLAX

Parallax is the angle that subtends at a given distance d using the radius of the Earth's orbit. For example, the distance from the star at the top of figure 1. The line of sight to the star is shown on the left, as seen from Earth at a given moment. Also, the star will have a particular apparent position in the sky. Six months later, for example, the parallax of the star will have changed. The star will appear at a different position in the sky. The angular difference between these two positions is called the parallax. Therefore, the parallax angle θ depends on both the radius of the Earth's orbit and the distance from the star.

In figure 1, we see that by applying the small-angle approximation to $\tan\theta = \frac{r}{d}$, which has a Taylor series $\tan\theta = \theta + \frac{\theta^3}{3} + \frac{2\theta^5}{15} + O(\theta^6)$, we obtain

$$\tan\theta \approx \theta = \frac{r}{d}\ \text{parallaxe}$$

UNITS	VALUE	SYMBOL	ABBREVIATIONS	RADIANS (APPROX.)
DEGREE	1/360 circle	°	deg	17.4532925 mrad
ARCMINUTE	1/60 degree	′	arcmin, ′, MOA	290.8882087 μrad
ARCSECOND	1/60 arcminute	″	arcsec, asec, as	4.8481368 μrad
MILLIARCSECOND	0.001 arcsecond		mas	4.8481368 nrad
MIRCO-ARCSECOND	0.001 mas		μas	4.8481368 prad

Units.

PARSEC

The *parsec* (symbol pc) is a unit of length used in astronomy for objects outside the solar system. The word parsec is a contraction of parallax-second. One parsec is defined as the distance at which one astronomical unit (au) subtends an angle of one arcsecond. One parsec is 3.085×10^{16} m, which is approximately 2.06×10^5 astronomical units ($(1/\tan(1''))$ au exactly), or 3.2616 light-years.

The angle theta in arcseconds is therefore equal to 1 over the distance in parsecs or

$$\theta[''] = \frac{1}{d[pc]}$$

One parsec is the distance from the sun to an astronomical object with a parallax angle of one arcsecond.

PLANETS

In our solar system, there are eight planets. We will express the mass of the terrestrial planets, which have a solid crust, in terms of the Earth's mass, and we will write the mass of the gas planets in terms of Jupiter's mass. The Earth's mass is

$$M_\oplus = 5.97 \times 10^{24} \text{ kg}$$

The Earth's radius is 6,371 km. The mass and the radii of the planets are often expressed in the units of Earth mass and Earth radius.

As well as the eight planets of the solar system, we currently know of 1,700 exoplanets or extrasolar planets. The first extrasolar planet was discovered in 1995 by Michel Mayol and Didier Qeloz at the Geneva Observatory.

COMETS

The solar system contains more than just planets. For example, there are comets, balls of ice and frozen mud that evaporate as they pass by the Sun. The material ejected by the comet nucleus is pushed into the shape of an enormous comet tail by the solar wind. The nucleus is usually tiny, at around 5 to 10 km in diameter, but ranges up to a maximum of 100 km for the largest comets. Comets are surrounded by a halo. The diameter of these halos ranges from 50,000 km to 250,000 km. The tail of a comet can be in the order of 60 to 100 million km in length. These sizes are therefore in the order of one astronomical unit.

Comets are composed primarily of organic matter; carbon, hydrogen, oxygen, and nitrogen. In fact, they are 80% water and approximately 10% carbon monoxide.

THE SUN AND THE STARS

The Sun is the only star that we know well. It is the only star whose surface we can see directly and photograph. Every other star is much too far away. The surface temperature of the Sun is 5,780°K. We can use the Sun's mass as a reference to describe the mass of other astronomical objects. Most large astrophysical objects are described in terms of the solar mass. The value of this solar mass is 2 × 10^{33} grams. The radius of the Sun, which we can also use to specify the radii of other stars, is 695,000 km, which is roughly 109 times the radius of the Earth.

Stars draw energy from two sources: gravitational contraction and the nuclear fusion reaction that transforms hydrogen into helium. When we refer to the lifetime of a star, we usually mean the period of time that it takes to burn all of its hydrogen into helium.

The mass of other stars can vary from 0.06 to 60 times the mass of the Sun. A mass of less than 0.06 times the solar mass is not enough to trigger a nuclear reaction. And if the mass is too large, i.e. 60 or even 100 times the solar mass, the star will collapse in upon itself and be destroyed.

PARAMETERS	RANGE	SUN
MASS	$0.06\ M_\odot < M_* < 60\ M_\odot$	2×10^{33} g
RADIUS	$0.17\ R_\odot < R_* < 15\ R_\odot$	695,000 km
TEMPERATURE	$2{,}640°K < T_* < 44{,}500°K$	5,780°K
LIFETIME	$5 \times 10^6\ ans < t_* < 10^{13}\ ans$	
LUMINOSITY	$1.2 \times 10^{-3}\ L_\odot < L_* < 8 \times 10^5\ L_\odot$	$3.846 \times 10^{26}\ W,\ 4 \times 10^{33}\ \mathrm{erg \cdot s^{-1}}$

The properties of stars.

If we compare radii, we find that that the radii of other stars range from 0.17 times to around 15 times the radius of the Sun.

The coolest stars have temperatures in the order of 2,640°K, and the hottest stars burn at temperatures in the order of 44,500°K.

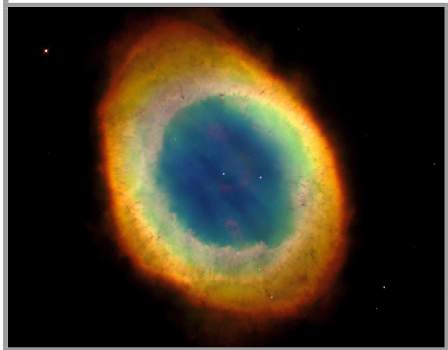

FIGURE 2

12:26 23:00

Messier 57, planetary nebula
(Image NASA/ESA-Hubble Heritage).

THE DEATH OF A STAR

Stars don't have an infinite lifetime. Once they have finished burning their hydrogen into helium, stars can die in one of two possible scenarios: either the initial mass of the star is more than 8 times the solar mass, which results in a supernova – the star explodes extremely violently – or its mass is less than 8 times the solar mass, which results in the formation of a planetary nebula.

In the centre of the planetary nebula, there is a star known as a *white dwarf* surrounded by the remnants of the original star.

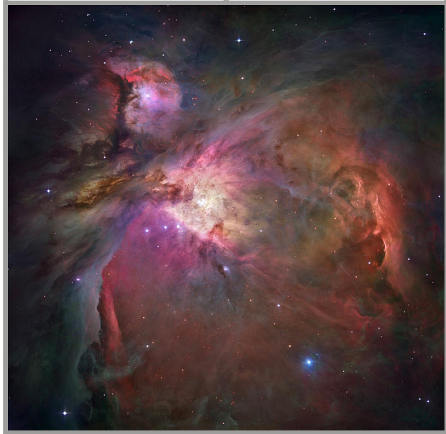

FIGURE 3

13:27 23:00

The Great Orion Nebula (Messier 42), with a cluster of young stars at its centre that are forming from the gas in the nebula (Image NASA/ESA-Hubble Heritage).

THE BIRTH OF A STAR

The material ejected after the death of a star, either in the form of a supernova or as a planetary nebula, is recycled into younger stars.

FIGURE 4

16:29 23:00

Omega Centauri, globular cluster (ESO image).

STAR CLUSTERS

There are multiple types of star cluster. There are clusters of young stars, open clusters, non-open clusters, and globular clusters, which have higher mass than open clusters. Open clusters have masses ranging from hundreds to thousands of solar masses. The mass of a globular cluster is in the order of 10^6 $M_\odot$. These clusters are composed of relatively old stars. These stars are generally between 10^9 and 10^{10} years old. They are found around the edges of galaxies. These clusters are larger than open clusters, with diameters of 40 to 50 parsecs.

FIGURE 5

17:25 23:00

NGC 4414, a spiral galaxy (Image NASA/ESA-STScl).

GALAXIES

Stars, planets, nebulae, and star clusters are all found in galaxies. The oldest stars are in the centre, and the younger stars tend to be found in the arms of the galaxy. Although it isn't visible in figure 5, there is a surrounding halo of dark matter in which the globular clusters can also be found.

The diameter of a galaxy is in the order of 30 to 40 kiloparsecs! Spiral galaxies have masses in the order of $10^9 - 10^{10}$ $M_\odot$. Our Milky Way is similar in appearance to the spiral galaxy shown in figure 5. The Sun is located at around two-thirds of the distance between the centre and the edge of the galaxy.

There are also elliptical galaxies, which are often located at the centre of a cluster of galaxies. Unlike spiral galaxies, these elliptical galaxies contain little or no dust. They also contain little or no gas, and very few stars form within them. Nevertheless, their mass varies over a larger range than the mass of spiral galaxies, between $10^7 - 10^{13}$ $M_\odot$.

FIGURE 6

21:09 23:00

Abell 1689, a galaxy cluster
(Image NASA/ESA-Hubble Heritage).

GALAXY CLUSTERS

There is often a primary elliptical galaxy at the centre of a galaxy cluster, with other elliptical galaxies further away from the centre. Galaxy clusters also contain spiral galaxies, and some from each category of galaxy. All of these galaxies orbit around a common centre of gravity. Galaxy clusters have the highest mass of all gravitationally bound structures in the universe. They do, of course, contain visible matter, but they are also immersed in a halo of dark matter, in the same way as single galaxies. The masses involved are absolutely enormous, from $10^{14} - 10^{15}\ M_{\odot}$. All of the astronomical objects that we have just encountered, from the smallest to the largest, with the least mass to the most mass, form part of a single whole - the universe, the study of which is called cosmology.

1.2 KEPLER'S THREE LAWS OF PLANETARY MOTION

1. The planets follow elliptical trajectories in a plane, with the Sun at one of the foci.
2. The area swept by the radius vector over a fixed period of time is constant: this is the law of areas.
3. The square of the orbital period of a planet is proportional to the cube of the semi-major axis of its orbit.

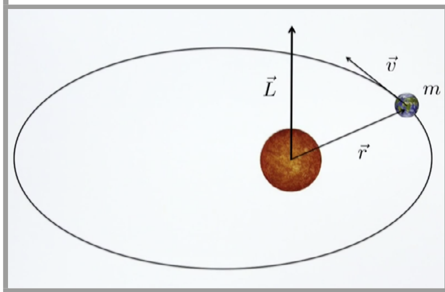

FIGURE 1

3:20 14:42

Orbit in a plane (Kepler's first law).

KEPLER'S FIRST LAW

First of all, it can be shown that the angular momentum $\boldsymbol{L}$ is constant:

$$\boldsymbol{L} = m\boldsymbol{v} \wedge \boldsymbol{r}$$

$$\frac{d\boldsymbol{L}}{dt} = m\underbrace{\frac{d\boldsymbol{v}}{dt}}_{=\boldsymbol{F}} \wedge \boldsymbol{r} + m\boldsymbol{v} \wedge \underbrace{\frac{d\boldsymbol{r}}{dt}}_{=\boldsymbol{v}} = 0 + 0 = 0$$

Since in the first term, the centripetal force $\boldsymbol{F}$ is collinear with $\boldsymbol{r}$, and in the second term $\boldsymbol{v}$ is obviously collinear with $\boldsymbol{v}$, both terms are zero, which implies that $\boldsymbol{L}$ is constant and that the orbit lies in a plane!

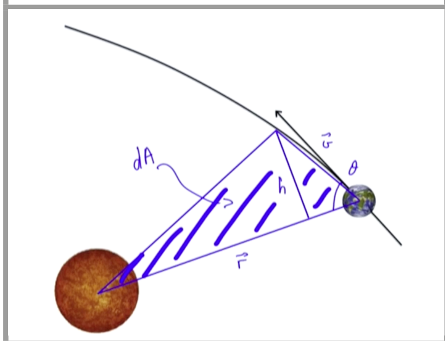

FIGURE 2

6:58 14:42

Area swept by the radius vector (Kepler's second law).

KEPLER'S SECOND LAW

The swept area dA is equal to the radius vector $\boldsymbol{r}$, which is given by the base of the triangle times the height h divided by two. We can write the height in terms of known quantities: the velocity, the angle, and the time required to travel this small distance along the Earth's orbit. Then

$$dA = \frac{1}{2}hr, \quad h = v\,dt\,\sin\theta$$
$$= \frac{1}{2}rv\,dt\,\sin\theta$$

and, since the angular momentum can be written

$$||\boldsymbol{L}|| = mvr\,\sin\theta, \quad \text{we can write}$$
$$dA = \frac{||\boldsymbol{L}||}{2m}dt$$
$$A = \int \frac{||\boldsymbol{L}||}{2m}dt = \frac{||\boldsymbol{L}||}{2m}t + C$$

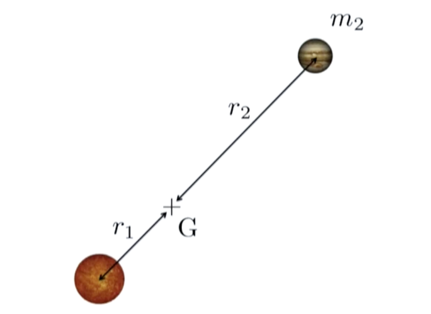

FIGURE 3
9:00 14:42
Reduced mass (Kepler's third law).

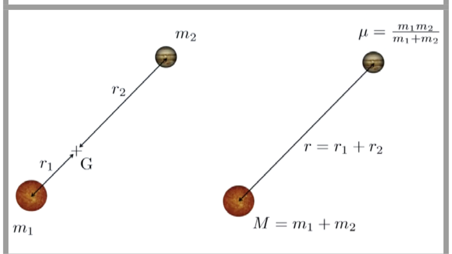

FIGURE 4
10:45 14:42
Reduced mass (Kepler's third law).

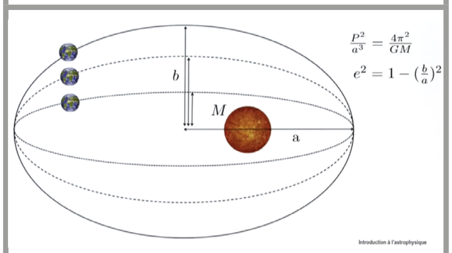

FIGURE 5
13:40 14:42
The period is independent of the eccentricity.

KEPLER'S THIRD LAW

To derive Kepler's third law in the special case of a circular orbit, consider a system of two masses m_1, m_2 orbiting at distances r_1 and r_2 around a common centre of gravity. The gravitational force between the two is

$$\begin{aligned} F_g &= G\frac{m_1 m_2}{(r_1+r_2)^2}, \quad \text{multiplying top and bottom} \\ &= G\frac{m_1 m_2}{(r_1+r_2)^2}\cdot\frac{m_1+m_2}{m_1+m_2} \\ &= G\frac{M\mu}{(r_1+r_2)^2}, \quad \mu = \frac{m_1 m_2}{m_1+m_2} \quad \text{the reduced mass} \end{aligned}$$

We thus obtain a system with fictitious mass M equal to the total mass of the planetary system.

We have reduced the system of motion of two bodies around a common centre of gravity to the motion of a single body μ, with fictitious mass, orbiting around another body to which we have assigned the sum of both masses of the bodies in the original planetary system. In a circular system, the acceleration of μ is related to the angular velocity as follows

$$a_\mu = \omega_\mu^2(r_1+r_2) = G\frac{M}{(r_1+r_2)^2}$$

We can replace ω_μ by $\frac{2\pi}{P_\mu}$ where P_μ is the period of the orbit to obtain:

$$\omega_\mu^2(r_1+r_2) = G\frac{M}{(r_1+r_2)^2}, \quad \omega_\mu = \frac{2\pi}{P_\mu}$$

$$\frac{4\pi^2}{P_\mu^2} = G\frac{M}{(r_1+r_2)^3} \quad \Rightarrow \quad \frac{P_\mu^2}{(r_1+r_2)^3} = \frac{4\pi^2}{GM}$$

For $m_1 \gg m_2 \quad \Rightarrow \quad M \cong m_1, \quad r \cong r_1$, so

$$P^3 = \frac{4\pi^2 r^3}{GM}$$

The eccentricity e of the orbit is defined by

$$e^2 = 1 - \left(\frac{b}{a}\right)^2$$

1.3 THE VIRIAL THEOREM

The *virial theorem* is to random motion what Kepler's laws are to motion in a plane: it relates the kinetic energy to the potential energy of "self-gravitating" systems, i.e. systems that only experience their own gravitational field and are isolated from any external gravitational fields.

The theorem applies to a stable, self-gravitating, spherical distribution of equal mass objects m with positions $\boldsymbol{r}$ and velocities $\boldsymbol{v}$ that experience the forces $\boldsymbol{F}$. It may be stated as:

$$\sum \frac{1}{2} m\overline{v^2} = -\frac{1}{2} \sum \overline{\boldsymbol{r} \cdot \boldsymbol{F}}$$

where the bar denotes the average time of the corresponding quantities.

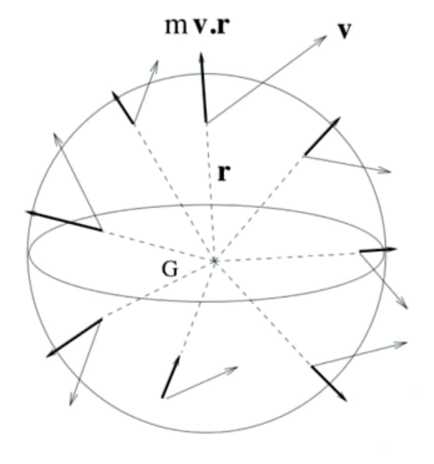

FIGURE 1

0:38 11:58

The virial theorem.

THE VIRIAL THEOREM

In a system in dynamic equilibrium, the kinetic energy K is equal to one half of the potential energy U, both of which are averaged over time:

$$2\langle K \rangle = \langle U \rangle$$

To derive the virial theorem, we begin by defining a quantity S representing the sum of the scalar product of the momenta of the particles with their position vectors:

$$\langle S \rangle = 0, \quad \frac{d\langle S \rangle}{dt} = \left\langle \frac{dS}{dt} \right\rangle = 0$$

Figure 1 shows the projection of all the momentum vectors onto the position vector for each particle. Since the position vectors are randomly distributed, and the velocities are also randomly distributed around the centre of gravity shared by all of the particles, S oscillates in time around an average value of zero. A fortiori, the derivative of this quantity also oscillates about the average value of zero. Therefore,

$$\left\langle \frac{dS}{dt} \right\rangle = \left\langle \sum_k \frac{\boldsymbol{p}_k}{dt} \cdot \boldsymbol{r}_k \right\rangle + \left\langle \sum_k \boldsymbol{p}_k \cdot \frac{\boldsymbol{r}_k}{dt} \right\rangle \Rightarrow$$

$$\left\langle \sum_k \frac{\boldsymbol{p}_k}{dt} \cdot \boldsymbol{r}_k \right\rangle = -\left\langle \sum_k \boldsymbol{p}_k \cdot \frac{\boldsymbol{r}_k}{dt} \right\rangle$$

$$\left\langle \sum_k \boldsymbol{F}_k \cdot \boldsymbol{r}_k \right\rangle = -\left\langle \sum_k m \cdot v^2 \right\rangle = -2\langle K \rangle$$

Next, we want to show that $\left\langle \sum_k \boldsymbol{F}_k \cdot \boldsymbol{r}_k \right\rangle$ is equal to the potential energy. We now know that there is a gravitational force $\boldsymbol{F}$ a force derived from potential energy, so we can also select this potential energy. Call this potential $\phi(r)$. We can assume that it will be proportional to some power of the radius, $n \cdot \phi(r) = -\alpha r^{(n+1)}$.

For gravity, $n = -2$, so the potential is proportional to $-1/r$ (recall that the potential energy of gravity is $U = G\frac{Mm}{r}$). We can thus rewrite this force as follows

$$\begin{aligned} \boldsymbol{F}_k &= m_k \frac{d\phi(r)}{dr} \cdot \frac{\boldsymbol{r}}{r} \\ &= m_k \left(-\alpha(n+1)r^n\right) \cdot \frac{\boldsymbol{r}}{r} \quad \text{so} \end{aligned}$$

$$\begin{aligned} \left\langle \sum_k \boldsymbol{F}_k \cdot \boldsymbol{r}_k \right\rangle &= -\left\langle \sum_k -m_k \alpha(n+1) r^{n+1} \right\rangle, \quad \text{and since} \quad n = -2 \\ &= \left\langle \sum_k +m_k \phi(r_k) \right\rangle = \langle U \rangle \end{aligned}$$

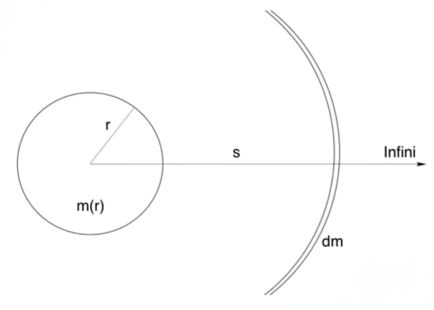

FIGURE 2

7:04 11:58

Potential energy of a sphere.

APPLICATION OF THE VIRIAL THEOREM

We can, for example, deduce the mass of objects from their potential energy ($\langle U \rangle$).

We can express the kinetic energy of a system in two different ways. For example, the kinetic energy of a gas cloud at a certain temperature may be expressed as $K \propto \frac{1}{2}nkT$ where k is the Boltzmann constant, n is the number of particles and T is the temperature *for each degree of freedom.*

R = Universal gas constant = 8.3145 J/molK
N_A = Avogadro's number = 6.0221 × 10^{23}/mol
$k = R/N_A$
k = Boltzmann constant = 1.38066 × 10^{-23} J/K = 8.617385 × 10^5 eV/K

Therefore, the kinetic energy in three dimensions is given by $K = \frac{3}{2}nkT$. Alternatively, it can be written as $K = \sum_k \frac{1}{2} m_k v_k^2$.

In order to express the potential energy of a body, we must simplify it greatly by assuming that it is a sphere of constant density ρ. We then stack spherical shells of density ρ from infinity to a specific radius r to form a body that ultimately has total mass (M) and radius (R), which is the final radius of the body once all of the shells have been stacked. The change in the potential energy associated with stacking the spherical shells is equal to the work carried out by gravity to bring a spherical shell from infinity down to radius r:

$$\begin{aligned} \delta U &= W_F(\infty \to r) \\ &= \int_\infty^r G \frac{m(r)dm}{s^2} ds \\ &= -G \frac{m(r)dm}{s} \Bigg|_\infty^r \\ &= -G \frac{m(r)}{r} dm \end{aligned}$$

To obtain the total potential energy, we must sum together all of the elementary potential energies that we just calculated, from 0 to the final value of the radius R of the star. Then, taking into account the fact that

$$M = \frac{4}{3}\pi R^3 \rho, \quad m(r) = \frac{4}{3}\pi r^3 \rho$$

we obtain the potential energy of a sphere:

$$\begin{aligned} U &= \int_0^R \delta U(r)\, dr \\ &= -\int_0^R G\frac{m(r)}{r} dm \\ &= -\int_0^R G\frac{m(r)}{r} 4\pi r^2 \rho dr \\ U &= -\frac{3}{5}\frac{GM^2}{R} \end{aligned}$$

Any astronomical object can be weighed. Its mass can be determined by measuring the velocity or velocity distribution and applying the virial theorem.

1.4 THE VIRIAL THEOREM: NUMERICAL ILLUSTRATIONS

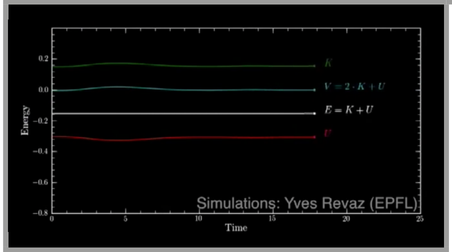

FIGURE 1

1:17 4:38

Simulation: Yves Revat, EPFL.

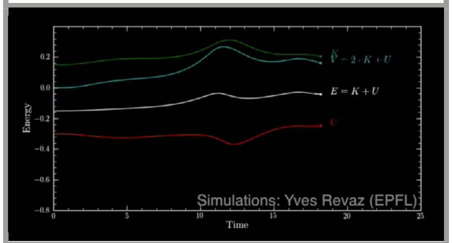

FIGURE 2

2:16 4:38

Simulation: Yves Revat, EPFL.

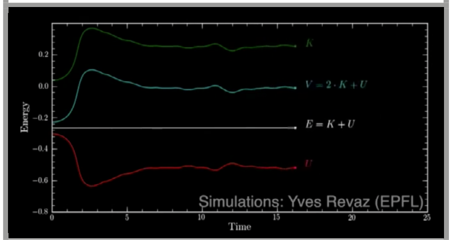

FIGURE 3

3:11 4:38

Simulation: Yves Revat, EPFL.

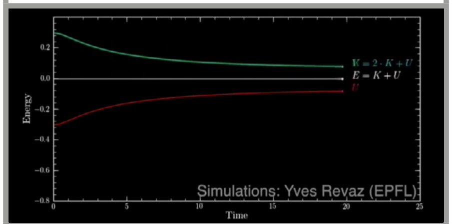

FIGURE 4

3:25 4:38

Simulation: Yves Revat, EPFL.

Using numerical simulations, we can describe the evolution of an isolated self-gravitating system of particles, i.e. acting under its own gravitational force. In these simulations, the initial positions of the particles are always kept exactly the same. Only the velocities are varied, which changes the kinetic energy of the system. At the bottom of each figure, the kinetic energy is shown in green, the changes in the potential energy is shown in red, and the sum of the two, i.e. the total energy, is shown in white. The virial is shown in blue. It is equal to twice the kinetic energy plus the potential energy.

Figure 1 shows a completely isolated system. We observe that the total energy is always conserved exactly, and that the potential energy plus twice the kinetic energy, known as the “virial”, does indeed oscillate around the mean value of zero over time.

In figure 2 the system is no longer isolated. A perturbation external to the system was introduced, which influences the shape of the self-gravitating system and the physical quantities measured. The system deforms, its total energy increases over time, and the virial no longer oscillates around zero, but increases over time.

Figure 3 shows an isolated system with initial conditions chosen in such a way that the kinetic energy is too low to balance the potential energy. In this example, the total energy is constant over time since the system is isolated, but the system will experience a contraction, causing the kinetic energy to rise sharply at the beginning of the simulation. Equilibrium will be achieved once the virial oscillates around zero.

Figure 4 shows an isolated system that contains too much kinetic energy relative to its potential energy. The kinetic energy is therefore going to decrease, whereas the potential energy will increase. The total energy will remain constant since the system is isolated. The virial will again converge towards an average around zero after a certain period of time.

2.1 THE PROCESS OF RADIATION

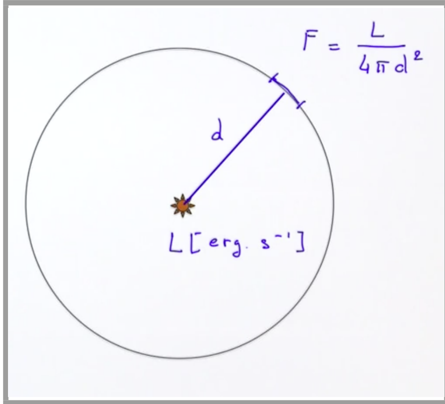

FIGURE 1

2:36 23:56

The measured energy is the same as that of a force.

PHOTONS: TRANSPORTING ENERGY

Photons are our only source of information from space. Their energy distribution and spectral distribution reveal information about the physical processes responsible for the emission and absorption of radiation, but also about the physical properties of the medium, i.e. the matter with which this radiation interacts.

$$E = h\nu = h\frac{c}{\lambda}$$

h: Planck's constant = 6.626×10^{-34} J · s
ν: photon frequency
λ: photon wavelength = $cP = c/\nu$

Light carries energy in the form of a wave or as a particle. This is known as wave-particle duality. Planck's constant has the same dimensions as the angular momentum. The frequency is related to the wavelength via the speed of light c and the oscillation period P of the wave, where $P=1/\nu$. If we consider a star radiating at a certain luminosity, L: the luminosity is, for example, measured in ergs per second, so units of energy over units of time, i.e. it is a force.

$$F_\lambda\text{: erg s}^{-1}\text{cm}^{-2}\text{A}^{-1}$$

$$F_\nu\text{: erg s}^{-1}\text{cm}^{-2}\text{Hz}^{-1}$$

$$1 \text{ erg} = 10^{-7} \text{ J}$$

This radiation is distributed over a sphere with surface area $4\pi d^2$ meaning that, from the ground, we ultimately see a stream of photons corresponding to an energy flux given by the original luminosity of the star divided by $4\pi d^2$.

Rewriting a flux expressed in terms of a wavelength in units of frequency is not as easy as just replacing λ by ν. No matter how the available energy is measured, we should obtain the same result: $F_\lambda d\lambda = -F_\nu d\nu$.

$$F_\lambda d\lambda = -F_\nu d\nu$$

$$\lambda = \frac{c}{\nu} \Rightarrow d\lambda = -\frac{c}{\nu^2}d\nu$$

$$F_\nu = \frac{c}{\nu^2}F_\lambda$$

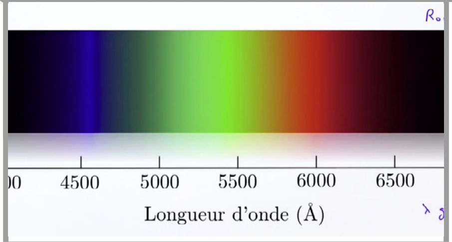

FIGURE 2

7:54 23:56

Continuous spectrum: continuous energy distribution.

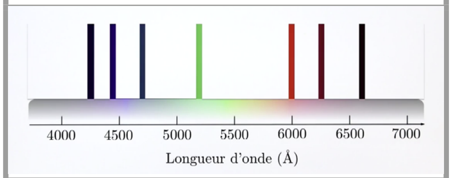

FIGURE 3

8:00 23:56

Line spectrum: discrete energy distribution.

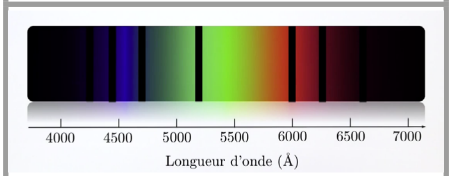

FIGURE 4

8:50 23:56

Continuous and discrete contributions.

PHOTONS: RADIATION PRESSURE

We can express the energy in terms of $E = h\nu$. We can also express it in terms of the famous mass-energy equation

$$
\begin{aligned}
E &= \sqrt{p^2c^2 + m^2c^4}, \quad \text{however photons do not have mass energy} \\
E &= \sqrt{p^2c^2 + \cancel{m^2c^4}} = pc, \quad \text{only motion energy} \quad \Rightarrow \\
p &= \frac{E}{c} = \frac{h\nu}{c}
\end{aligned}
$$

If a photon collides with a particle of matter and is absorbed, the momentum of the photon is transferred to the particle. The following then holds for the particle:

$$\frac{dp}{dt} = \frac{h\nu}{c} = \|\boldsymbol{F}\|$$

This force is extremely important in astrophysics. It drives the creation of stars by causing clouds of atoms or molecules to collapse. This force is called the *radiation pressure*. It is the force generated by a flux of photons on a collection of particles, atoms, molecules, or dust.

In most cases, astronomical objects have spectra that combine both types of radiation, continuous radiation and discrete radiation (line spectra). Different physical processes are responsible for each type of emission, which is precisely what allows us to study the stars. The energy distribution of photons in atomic and molecular clouds is discrete. In both the continuous and discrete cases, certain wavelengths are absorbed (fig. 4).

Every star has this type of spectrum: one continuous component originating from the fact that the surface is heated by the nuclear reactions unfolding inside, and possibly also absorption lines at the surface due to the cooler hydrogen in its atmosphere.

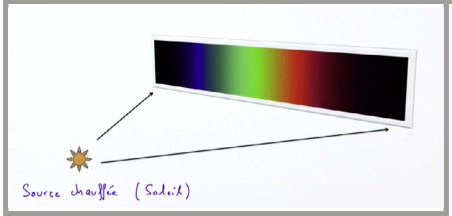

FIGURE 5(A)
10:05 23:56
Continuous spectrum.

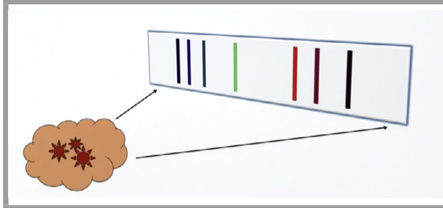

FIGURE 5(B)
10:14 23:56
Discrete spectrum.

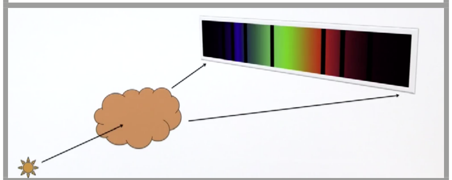

FIGURE 5(C)
11:09 23:56
Continuous and discrete spectrum.

CONTINUOUS RADIATION

Which processes emit continuous radiation?

- The Sun and stars emit a black-body spectrum (*black-body radiation*).
- Compton scattering (Bremmstrahlung radiation), which takes place in ionized gases within galaxy clusters.
- Synchrotron radiation occurs when there are magnetic field lines running through the interstellar medium, within the intergalactic medium or around astronomical objects.

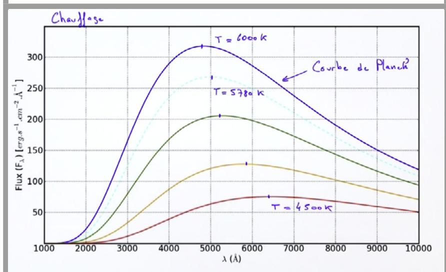

FIGURE 6
16:43 23:56
Black-body radiation.

BLACK-BODY RADIATION

This is continuous type of radiation emitted by heat sources. The spectrum of a black body is a Planck curve with the defining property that the emission peak depends solely on the temperature. Cooler black bodies have radiation peaks closer to the red end of the spectrum. Hot stars tend to be bluer, whereas cooler stars tend to be redder. This phenomenon can also be observed in hot gases such as plasmas.

COMPTON SCATTERING

This radiation arises when a proton gas is ionized by high-speed electrons. Every time an electron passes near a photon, it is accelerated, and emits a photon in a random direction. This radiation is *isotropic* and plays an important role in objects with very high masses where heat is generated by gravitational contraction, for example galaxy clusters. This creates plasmas where electrons interact with ions, and whenever there is an acceleration, which is generally uniformly distributed or at the very least continuous, the emitted photons will also have continuous energy distributions. The spectrum itself is therefore also continuous.

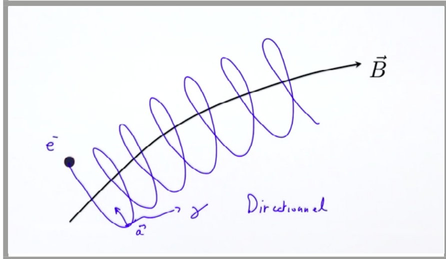

FIGURE 7

19:53 23:56

Electrons spiralling around the magnetic field lines.

FIGURE 8

21:05 23:56

The same nebula viewed with optical radiation and optical radiation plus X-rays (image NASA/ESA/HST/ASU/J. Ester *et al.*)

SYNCHROTRON RADIATION

This is the same kind of radiation as can be observed in particle accelerators. When the magnetic field induces a centripetal acceleration on the electrons, photons are emitted. In this case, the electrons are emitted in a certain direction, which is the same direction as the magnetic field, and not scattered as in Compton radiation. Compton radiation also requires heat to separate the atoms into electrons and ions, which makes it an example of "thermal" radiation. The magnetic field, on the other hand, doesn't require extreme temperatures. This effect can occur even at extremely low temperatures. It is an example of "non-thermal" radiation.

In the same way that the intensity of Compton radiation depends on the temperature and electron density, synchrotron radiation depends on the intensity of the magnetic field and the electron density. Therefore, whenever this type of radiation is observed, the observed luminosity provides information about the intensity of the magnetic field present at a given location, as well as the electron density.

By studying the optical radiation, we can measure the chemical composition of the gas surrounding supernovae, and calculate the speed of expansion of the nebula. The X-ray emissions provide information about the plasma density, i.e. the electron and ion gas, and the intensity of the magnetic field in nebulae.

2.2 BLACK BODIES/ATOMIC LINES

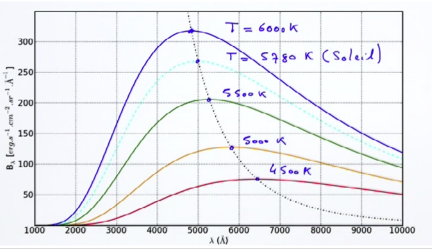

FIGURE 1

2:38 20:15

Peak emission wavelength (Wien's displacement law).

The *luminance* of a black body is a function of its wavelength or frequency. As a function of the wavelength,

$$B_\lambda = \frac{2hc^2}{\lambda^5} \cdot \frac{1}{e^{hc/\lambda kT} - 1}$$

Luminance is measured using units of power per unit area, per square radian in the case of radiation emitted in all directions or, alternatively, per unit wavelength or per unit frequency $\left[\mathrm{erg} \cdot \mathrm{s}^{-1} \cdot \mathrm{cm}^{-2} \cdot \mathrm{sr}^{-1} \cdot \mathrm{Å}^{-1}\right]$.

As a function of the frequency, we have the following equation per unit frequency:

$$B_\lambda = \frac{2h\nu}{c^2} \cdot \frac{1}{e^{hc/\lambda kT} - 1} \quad \mathrm{erg} \cdot \mathrm{s}^{-1} \cdot \mathrm{cm}^{-2} \cdot \mathrm{sr}^{-1} \cdot \mathrm{Hz}^{-1}$$

WIEN'S DISPLACEMENT LAW

Wien's displacement law, which gives the peak value of black body radiation as a function of the temperature, may be expressed in terms of the wavelength or the frequency depending on whether we are considering the luminance as a function of wavelength or of frequency.

$$B_\lambda = \frac{2h\nu^3}{c^2} \cdot \frac{1}{e^{hc/\lambda kT} - 1}$$

$$\lambda_{\max} T = 2.9 \times 10^{-3}\ [\mathrm{m{\cdot}K}]$$

$$\lambda_{\max} T = 2.9 \times 10^{7}\ [\mathrm{Å{\cdot}K}]$$

$$\nu_{\max}/T = 5.9 \times 10^{10}\ [\mathrm{Hz{\cdot}K^{-1}}]$$

$$\lambda_{\max} T \cdot \frac{\nu_{\max}}{T} = \lambda_{\max} \cdot \nu_{\max} = 0.57c$$

The final equation on the right is a result of the fact that B_ν is not equal to B_λ, but is instead equal to $B_\lambda \cdot \frac{d\lambda}{d\nu}$ as was shown earlier, and therefore $B_\nu = B_\lambda \cdot \frac{\lambda^2}{c}$.

ENERGY FLUX DENSITY

The density of the energy flux arising from an object emitting black-body radiation is given by the integral of the luminance over all wavelengths or at all frequencies. The value of this integration is the energy flux density, which is proportional to the fourth power of the black body's thermodynamic temperature. The coefficient of proportionality σ is a power per unit surface area and per Kelvin to the power of four. M simply represents the energy per unit time, or in other words the power generated at the surface of the black body.

$$M = \sigma T^4$$

$$\sigma = 5.67 \cdot 10^{-11}\ \mathrm{erg} \cdot \mathrm{s}^{-1} \cdot \mathrm{cm}^{-2} \cdot K^{-4}$$

LUMINOSITY OF A STAR

The luminosity is the total energy released by the star, in erg/second. This is therefore equal to the surface area of a body of radius r times M.

$$L = 4\pi r^2 \cdot M$$
$$= 4\pi r^2 \cdot \sigma T^4$$

The luminosity is integrated over the whole surface, whereas M is the available energy per unit surface area on the surface of the black body. On Earth, at a distance d away from the body, we only receive a fraction of this energy in the form of a flux per unit surface area. The flux F is given by L spread over a sphere of radius $4\pi d^2$:

$$F = \frac{L}{4\pi d^2} \quad \mathrm{erg \cdot s^{-1} \cdot cm^{-2}} \quad \text{ou}$$
$$F = \frac{L}{4\pi d^2} \quad \mathrm{erg \cdot s^{-1} \cdot cm^{-2} \cdot \AA^{-1}}$$

from the perspective of spectroscopy and when the light is dispersed as a function of the wavelength.

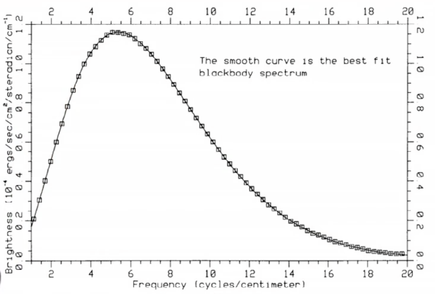

FIGURE 2

8:20 20:15

Microwave spectrum measured by the COBE satellite, Cosmic Background Explorer (Image credit: Mather *et al.*, 1990, *Astrophysical Journal*354, L37).

COSMIC MICROWAVE BACKGROUND

The cosmic microwave background, the spectrum of which is shown in figure 2 as a function of frequency, is an isotropic form of microwave radiation present everywhere in the universe, originating from the Big Bang. The universe, originally extremely hot, expanded and then cooled, emitting ambient radiation which is currently, 13.7 billion years after the Big Bang, equivalent to a black body with temperature extremely close to absolute zero: 2.73°K.

THE HYDROGEN ATOM

Given the Bohr model of an atom as electrons orbiting around protons, we can define the Coulomb force as the centripetal force experienced by the electron:

$$\boldsymbol{F}_c = \frac{e^2}{4\pi\varepsilon_0 r^2} = \frac{mv^2}{r} = m\boldsymbol{a}$$

where ε_0 is the permittivity of free space. Quantum mechanics tells us that momentum is quantized, and that the angular momentum is equal to an integer times a constant. This means that

$$mvr = n\hbar \quad \left(h = 6.626\times10^{-34}\,\mathrm{m}^2\cdot\mathrm{kg}\cdot\mathrm{s}^{-1}, \quad \hbar = \frac{h}{2\pi} \right)$$

These equations allow us to calculate the total energy of the electron.

$$\begin{aligned} E_{total} &= \underbrace{\frac{1}{2}mv^2}_{\text{kinetic energy}} - \underbrace{\frac{1}{4\pi\varepsilon_0}\frac{e^2}{r}}_{\text{potential energy}} \quad \text{as a function of } n \text{ and } h \quad \Rightarrow \\ &= -\frac{me^4}{32\pi^2\varepsilon_0^2\hbar^2}\cdot\frac{1}{n^2} \end{aligned}$$

The total energy thus depends on some integer and some constant. This constant is $C = -2.18\times10^{-18}\ \mathrm{J} = -13.6\ \mathrm{eV}^1$. We therefore see that each orbit n is characterised by its angular momentum and its energy.

$$E_n = -13.6\times\left(\frac{1}{{}^2}\right)\ \mathrm{eV}$$

Electrons can move between orbits by gaining or releasing energy. Energy is released in the form of a photon with frequency

$$E_{n1} - E_{n2} = -13.6\times\left(\frac{1}{n_1^2} - \frac{1}{n_2^2}\right)\ \mathrm{eV} = \mathrm{h}\nu$$

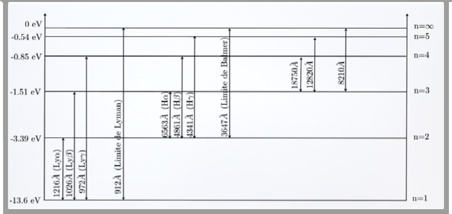

FIGURE 3

16:53 20:15

Atomic lines of hydrogen.

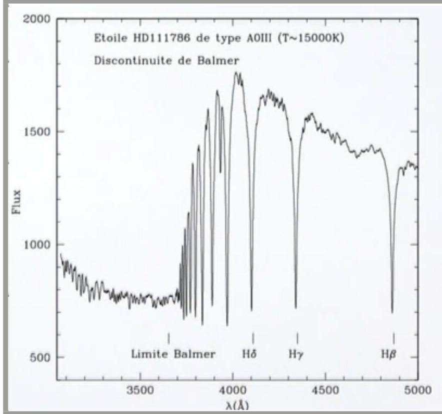

FIGURE 4

17:16 20:15

The star HD111786, with a temperature of $T \approx 15000\ ^\circ K$.

THE ATOMIC LINES OF HYDROGEN

The Lyman series lists all possible transitions between the lowest energy level and every other energy level that the atom can take. If an energy greater than 13.6 eV is applied to the atom, it becomes ionized. In other words, it loses its electron. Ionized gas is therefore gas that has been converted into ions and electrons. The wavelengths needed to facilitate this ionization are found towards the ultraviolet end of the spectrum. If the electron drops from level $n = 2$, we obtain the so-called *Balmer series*, describing the release of photons in the visible range.

By studying the star HD111786, which has a temperature of $T \approx 15000\ ^\circ K$, we can observe discontinuities in the Balmer series within the visible spectrum. The hydrogen gas cloud surrounding the star is ionized and these wavelengths are absorbed by the gas, which creates the visible pattern shown in figure 4.

2.3 MEASURING RADIATION

Radiation can be collected by telescopes or antennae, depending on the wavelength of the radiation to be observed. The observatory can be located at ground level if the atmosphere does not interfere too strongly with radiation originating from the stars, otherwise it must be placed in space. We will see later how astronomers measure the luminous flux, the colour of stars, and finally the luminosity of the stars.

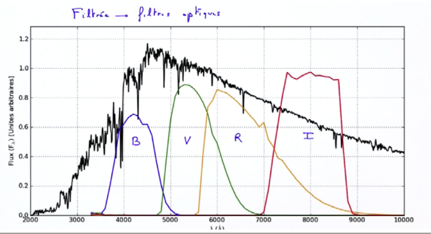

FIGURE 1

1:54 20:37

Example of a stellar spectrum (black) with optical bandwidth filter overlays B = blue; V = visible green; R = red; I = infrared.

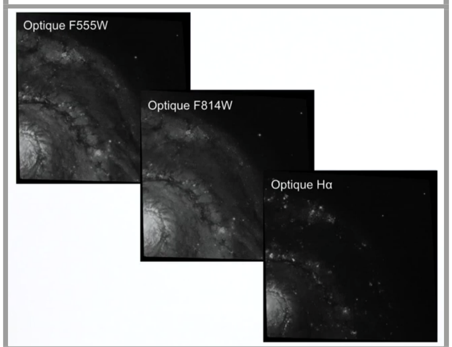

FIGURE 2

5:10 20:37

Region of the spiral galaxy M51, viewed through three different filters (image: NASA/ESA-STScI).

FIGURE 3

5:10 20:37

Colour image generated from 3 images taken using 3 different filters (image : NASA/ESA-STScI).

THE ANALYSIS OF LIGHT

We can analyze light using filters to isolate certain ranges of wavelength. There are filters for wavelengths outside of the spectrum that can be perceived by the human eye. By integrating values over all wavelengths that pass through a given filter, we obtain the flux in this bandwidth. This flux, associated with a specific bandwidth, then allows us to build up a picture of the luminosity at specific wavelengths.

Filter A at 5,555 angströms filters out blue phenomena, such as young and host stars with high mass. Filter B at 8,140 angströms filters out red phenomena, such as older stars. C filter captures the hydrogen lines $H\alpha$ at 6,563 angströms, which are typical of star formation. The luminosity of the three images is then rendered in RGB, with the first coloured in blue, the second in green, and the third in red, which creates a colour image. Combining these three images shows young stars in the star formation zone in blue, and the zones of gases ionized by high-mass stars in red.

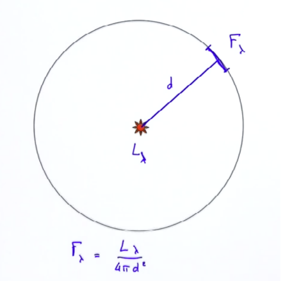

FIGURE 4

9:21 20:37

Magnitude systems and the effect of distance on the observed luminous flux.

MAGNITUDE SYSTEMS

The luminous flux at a certain wavelength F_λ may be deduced from the luminosity at this wavelength using:

$$F_\lambda = \frac{L_\lambda}{4\pi d^2} \quad \left[\mathrm{erg \cdot s^{-1} \cdot cm^{-2}}\right]$$

However, to be consistent with what ancient astronomers recorded, and taking into account the nature of the eye, which responds to changes in light intensity on a logarithmic scale, astronomers ultimately decided to measure the luminous flux not as a flux, but as a magnitude on a logarithmic scale.

$$m_\lambda = 2.5 \log F_\lambda$$

The flux scale is calibrated to the star Vega, an extremely bright star in the northern hemisphere, whose magnitude is defined to be zero with respect to the V filter (visible green). In other words, to find the magnitude of a star, we must find the difference between its flux and the flux of Vega on a logarithmic scale:

$$\begin{aligned} m_{star} - m_{vega} &= -2.5\log(F_{star}) + 2.5\log(F_{vega}) \\ &= -2.5\log\left(\frac{F_{star}}{F_{vega}}\right) \quad \text{and since } m_{vega} = 0 \text{ by definition} \\ m_{star} &= -2.5\log\left(\frac{F_{star}}{F_{vega}}\right) \end{aligned}$$

THE COLOUR OF STARS

We can also measure the slope of the spectrum between two bands for the same object. This slope is also calibrated to the corresponding flux ratio of Vega between the same two bands. For example, we can find the slope between the V band and the I band of an object

$$\begin{aligned} m_V - m_I &= -2.5\log\frac{F_V(obj)}{F_V(Vega)} + 2.5\log\frac{F_I(obj)}{F_I(Vega)} \\ &= -2.5\log\frac{F_V(obj)}{F_I(obj)} + 2.5\log\frac{F_V(Vega)}{F_I(Vega)} \end{aligned}$$

This is simply the difference between the magnitude of the objective divided by the magnitude of Vega at each of the bands V and I. Usually, to denote the colour indices, we write *V-I* and *B-V* in place of $m_V - m_I$ and $m_B - m_V$. The bluest filter is also always placed "on the left". With this convention, large colour indices are typical of red objects, and low colour indices are characteristic of blue objects.

ABSOLUTE MAGNITUDE AND THE DISTANCE MODULUS

The absolute magnitude M is a separate concept from the visual magnitude m. It represents the magnitude of the object as viewed from a distance of 10 parsecs. The surface area over which the luminosity is spread is normalized when measuring the flux. Thus

$$\begin{aligned} m &= -2.5\log F \\ m - M &= -2.5\log\frac{L}{4\pi d^2} - 2.5\log\frac{L}{4\pi 10^2} \\ &= -2.5\log\frac{10^2}{d^2} \\ m - M &= 5\log d - 5, \quad \text{the distance modulus} \end{aligned}$$

This result is essential, as it allows us to measure distances using the standard candles approach. In the table below, the lowest values denote the brightest stars. The absolute magnitude of the Sun, viewed at 10 parsecs, is therefore the lowest value.

OBJET	m	M
SUN	-26.8	+4.8
FULL MOON	-12	invisible
VENUS	-4	invisible
BETELGEUSE (SUPERGIANT)	0.5	-5.6
ANDROMEDA GALAXY	3.4	-20.7
VERY DISTANT QUASAR	25-28	-30

Orders of magnitude.

3.1 THE DOPPLER EFFECT

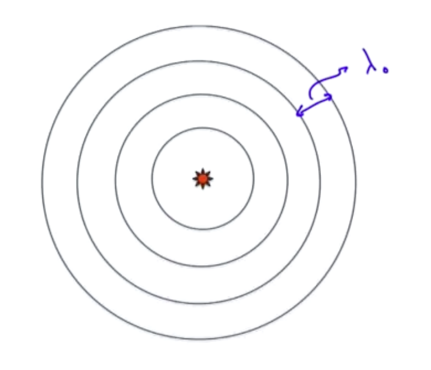

FIGURE 1(A)

1:28 23:47

Emission of spherical waves by a body at rest.

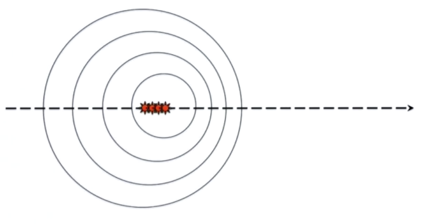

FIGURE 1(B)

2:14 23:47

Emission of spherical waves by a moving object.

The Doppler effect allows us to measure the velocity of stars and, therefore, study their motion. For example, if used in combination with the virial theorem and Kepler's laws, both of which are based on velocity, we can indirectly measure the masses of stars. This effect is the results of two kinds of motion: if a source is moving relative to an observer while emitting a sound or light wave, the observer will see a shorter wave if the source is moving towards the observer, i.e. blue shift, and a longer wavelength if the source is moving away from the observer, which results in redshift .

When the star is at rest, the time between wave fronts Δt_0 is equal to the period of the wave.

When the star is moving *towards the observer*, Δt is the period between two successive wave fronts are seen by the observer. Then

$$\begin{aligned}\Delta t &= \Delta t_0 - \frac{\Delta x}{c} \\ &= \Delta t_0 - \frac{v}{c}\Delta t_0, \quad \lambda = c\Delta t \\ \lambda_{\text{perceived}} &= \lambda_0 - \frac{v}{c}\lambda_0 \quad \text{towards the observer}\end{aligned}$$

Generalising this formula to include cases where the star is moving at an angle to the observer, we obtain:

$$\lambda_{\text{perceived}} = \lambda_0 - \frac{v}{c}\lambda_0 \cos\theta$$

where θ is the angle between the path of the star and the line of sight of the observer. We can rearrange this equation as follows:

$$\frac{\lambda_{\text{perceived}} - \lambda_0}{\lambda_0} = -\frac{v}{c}\cos\theta = z = \textit{redshift}$$

$$\lambda = \lambda_0(1+z)$$

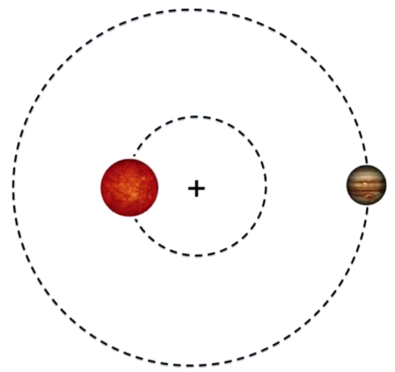

FIGURE 2(A)

16:52 23:47

Examples of applications used for the search for exoplanets.

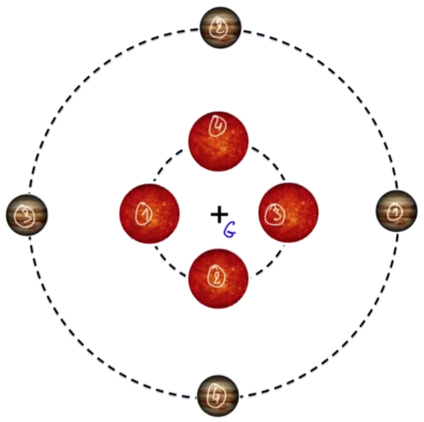

FIGURE 2(B)

18:27 23:47

Examples of applications used for the search for exoplanets.

MEASURING REDSHIFT

In the field of optics, a spectrograph can be used to split incoming light according to its wavelength so that the resulting spectrum can be recorded by a sensor. In the field of astronomy, a mask with a slit in it is mounted at the centre of the telescope, and the light coming through the slit is split by a prism to obtain an image for each wavelength.

This technique can be used to measure the speed of objects with emission lines, as well as the speed of objects that absorb background radiation and the rotational velocity of rotating objects. One extremely important application of spectroscopy in astrophysics is in the search for exoplanets where it is used to measure the radial velocity of stars orbited by planets outside of our solar system. This is extremely difficult in practise, since the distance between a star and its planet is extremely small, and the contrast in luminosity between the star and its planet is extremely large.

Figure 2(b) shows four positions of a star and a planet orbiting around their common centre of gravity. The star has an apparent angular velocity of $v_{max}\sin\theta$, since the planet being measured could potentially be orbiting at an inclined angle relative to the celestial plane. The planet is not visible in the spectra of this system. Only the star is visible due to the oscillations in its velocity as it orbits around the common centre of gravity of the star-planet system. Over time, the curve traced out by the radial (angular) velocity produces a period T and an amplitude, which gives the component v_{max} parallel to the line of sight of the velocity of the star. Stellar evolution theory can then be used to deduce the mass M of the star from its spectrum.

HUBBLE'S LAW: THE EXPANSION OF THE UNIVERSE

The distance between galaxies is increasing over time. No matter which galaxy we look at, it appears to be moving away from us. This phenomenon is measured by Hubble's law, which describes the recession velocity of a galaxy. The radial velocity of these galaxies is also proportional to the distance.

$$v_{gal} = H_0 d$$

where H_0 is the coefficient of proportionality and d is the distance modulus. The radial velocity is measured using the Doppler effect and d is measured using the distance modulus.

3.2 INTERSTELLAR AND INTERGALACTIC MATTER

FIGURE 1

0:33 32:24

Planetary nebula NGC 2392 (image: NASA/ESA, C.R. O'Dell).

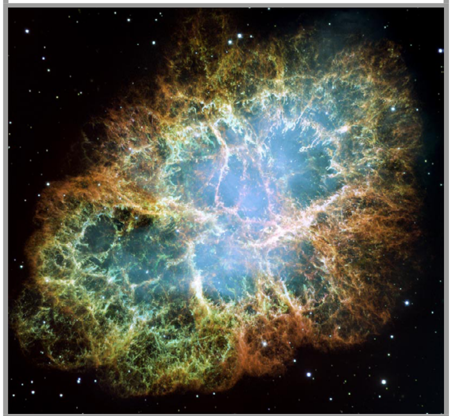

FIGURE 2

0:45 32:24

M1 Nebula, supernova residue (image: NASA/ESA).

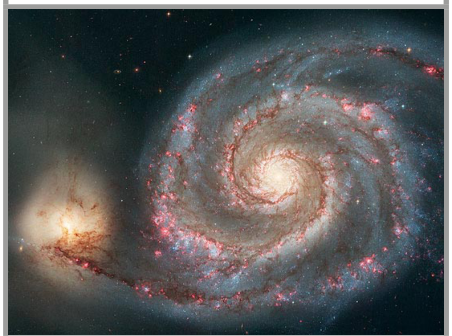

FIGURE 3

1:03 32:24

M51 galaxy (image : NASA/ESA).

Cosmic gas, excluding the primordial hydrogen and helium that formed in the moments following the Big Bang, is produced by successive generations of stars. When a star dies this gas is ejected into the interstellar medium. If the star has low mass, less than 8 times the solar mass, a planetary nebulae is created (fig. 1). If the mass of the star is more than 8 times the solar mass, the result will be supernova explosions (fig. 2). The both cases, the gas products are recycled in the interstellar medium.

Galaxies also contain dust. This dust absorbs the background radiation, creating black trails that can be seen through the spiral arms of the Messier 51 galaxy (fig. 3). This dust, mixed with gas, will create the next generations of stars, and possibly also planetary systems like our own.

FIGURE 4

3:31 32:24

Carina Nebula (image: NASA/ESA).

DETAILED EXAMPLE OF A NEBULA

In the Carina Nebula (fig. 4) viewed with optical radiation, we can identify a few sources of ionization in the form of hot, young stars. Between these stars, there is gas that will split into electrons and protons by ionization. This gas can potentially reform, which causes the electrons to de-energize and occupy the lower energy levels, releasing photons.

The gas between young stars has very low density, in the order of one particle per square centimetre or, in terms of mass density, $\rho = 10^{-21}$ kg/m^3. The black part of figure 4 shows how the dust absorbs radiation. The density of the dust is even lower, at 10^{-13} particles per cm^3. However, the dust particles are much heavier. The mass density is closer to the order of 10^{-23} kg/m^3. So, there are 13 orders of magnitude fewer particles than in the gas, but the mass density is only 100 times smaller.

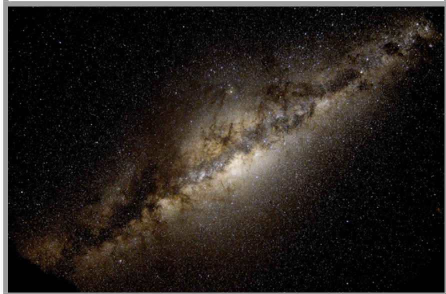

FIGURE 5

4:00 32:24

The Milky Way (image: ESO).

THE MILKY WAY

The scale is much larger than in the case of a nebula. Nevertheless, the dust (shown in black in figure 5) extends over large regions. We can conclude that dust and gas play an important role at absolutely every scale.

THE STRÖMGREN SPHERE

After being ionized by the stars, the interstellar gas tends to recombine, emitting light. The equilibrium between the tendency to ionize and the tendency to recombine determines the radius of the sphere. The limiting radius for the size of a nebula determined by this equilibrium is called the *Strömgren radius*. At the Strömgren radius, the flux of ionizing photons is equal to the rate of recombination of electron-proton pairs. Its value is the volume of the nebula $\left(\frac{4}{3}\pi r^3\right)$ multiplied by the number of available electron-proton pairs ($N_{ion} = N_{recombinaison}$).

$$N_{recombinaison} = \frac{4}{3}\pi R^3 n_e n_H \alpha$$

where R is the radius of the nebula, n_e is the number of available electrons, n_H is the number of available protons, and α is a physical constant equal to $\alpha = 3\times10^{-13}\mathrm{cm}^3\cdot\mathrm{s}^{-1}$ for a gas at the typical temperature of 8,000°K.

To calculate the number of ionizing photons, we can consider a typical star with a temperature of approx. 45,000°K as the ionization source. The black-body spectrum of this star peaks in the ultraviolet region at λ_{max} 640$\mathring{A}$ in accordance with Wien's law. Since the peak radiation of this ionizing star is at 640$\mathring{A}$, each photon has an energy of $E_\gamma = h\nu \approx 19$ eV. This ionization energy is higher than the threshold of 13.6 eV, so all of the hydrogen of the nebula is ionized. Therefore $n_e = n_H$, so:

$$N_{recombinaison} = \frac{4}{3}\pi R^3 n_H^2 \alpha = N_{ion} \Rightarrow R_s = \left[\frac{3N_{ion}}{4\pi\alpha n_H^2}\right]^{\frac{1}{3}}$$

The HI atom has the electron with the lowest energy level, namely –13.6 eV. The hydrogen must therefore receive 13.6 eV in order to be ionized.

SYMBOL	MEANING
^1H	a hydrogen nucleus
^2H	a deuterium nucleus
HI	a neutral hydrogen atom
HII	an ionized hydrogen atom
Hα, Hβ, Hγ	hydrogen emission lines
H_2	molecular hydrogen

The nomenclature of hydrogen.

We can estimate the number of ionizing photons from the luminosity of the ionizing star.

$$N_{ion} = \frac{L_*}{E_\gamma}$$

For a star with T_* = 45,000°K, the luminosity is L_* = 1.3 · 10^5 L_* (the solar luminosity). A few calculations allow us to calculate the number of ionizing photons, which is 1.6 · 10^{49} photons per second. For example, if we make the estimate n_H = 5,000 particles/cm^3, we find a radius $R \approx$ 0.3 pc. The nebulae of small clusters of stars typically have a radius of 0.1 < R_S <100 pc.

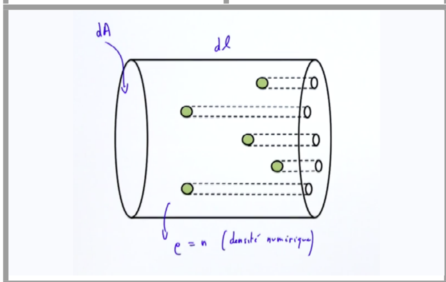

FIGURE 6

14:42 32:24

Illustration of the absorption of light by dust particles.

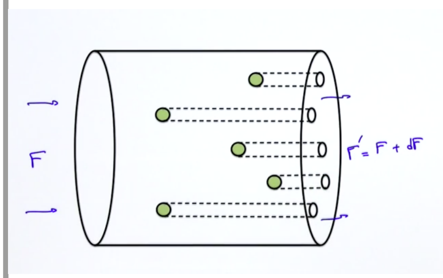

FIGURE 7

16:35 32:24

Illustration of the absorption of light by dust particles.

OPTICAL DEPTH

In the volume element shown on the right of figures 6 and 7, given a radius r for the dust particles (shown in green in the figure), each particle has an extinction coefficient of $C_{ext} = \pi r^2$. Therefore, the fraction of the surface hidden by all of the dust particles $d\tau$ is

$$\begin{aligned} d\tau &= \frac{n\, dA\, dl\, C_{ext}}{dA} \\ &= C_{ext} n\, dl \\ \tau &= \int_0^D C_{ext} n\, dl \quad \text{where } D \text{ is the distance to the star} \\ &= \overline{n} C_{ext} D \end{aligned}$$

where $\overline{n}$ is the average number of particles along the line of sight. We integrate the radiation lost as a result of this average number of particles on each volume element as far as the source that we are observing. The parameter τ is the *optical depth*, which is a dimensionless number. τ=1 corresponds to total absorption. To estimate the fraction of the flux that is lost, assuming the flux enters from the left, we can write

$$\begin{aligned} F' &= F + dF \quad (dF \leq 0) \\ dF &= -F\, d\tau \quad \Rightarrow \quad \frac{df}{F} = -d\tau \\ F &= F_0 e^{-\tau(D)} \end{aligned}$$

To express this extinction as a magnitude, we calculate the magnitude of the observed star minus the magnitude of the star prior to absorption by the dust.

$$\begin{aligned} m - m_0 &= -2.5 \log \frac{F(D)}{F_0} \\ &= 2.5\tau(D) \log e \end{aligned}$$

FIGURE 8
25:34 32:24

M78 nebula by reflection (image: ESO).

ABSORPTION, SCATTERING, REFLECTION

Absorption is not the only phenomenon that occurs within each volume of the gas. Some photons can be reflected straight back, whereas others can be deflected in random directions. This is known as *scattering*. There are two types of scattering.

Mie scattering occurs when the radius of the particle is much larger than the wavelength being observed. In this case, the extinction coefficient of this Mie scattering is proportional to $1/\lambda : C_{ext} \propto \lambda^{-1}$. This scattering is also *directional*. This means that the photons are not deflected randomly. Instead, they are redirected in the direction closest to the direction of incidence.

Another type of scattering is *Rayleigh scattering*, which occurs when the radius of the particles is smaller than the wavelength being observed.

MIE SCATTERING: $r \gg \lambda$

$$C_{ext} \propto \lambda^{-1}$$

Directional

RAYLEIGH SCATTERING: $r \ll \lambda$

$$C_{ext} \propto \lambda^{-4}$$

Isotropic

At the centre of the nebula on the right of figure 8 (M78 in the Orion constellation), there are stars hidden behind dark patches of light-absorbing dust. The light is scattered in the brightest zones. When we look at the spectrum of a star, we see a black body. When we look at the spectrum of a nebula, we might expect to see a line spectrum, since the atoms can be ionized by the stars, creating emission lines when they recombine. But this is not necessarily the case. In fact, some stars fail to ionize the matter. Instead, the matter scatters light, producing a continuous black-body spectrum. So, when scattering dominates, we observe a black-body spectrum, and when ionization and recombination dominate, we observe a line spectrum.

Therefore, whether scattering or absorption dominates depends on the wavelength. Both processes are more effective at shorter wavelengths. This has two consequences:

– Fainter objects that produce less light than they intrinsically emit are easier to see.
– The absorption or scattering of light increases as the wavelength becomes smaller, so objects appear redder when viewed through dust.

This means that in order to see objects whose light is strongly absorbed, we must observe them in the infrared spectrum.

COLOUR INDEX

The colour index of a star is the difference between the apparent magnitudes of two different spectral bands, for example $(B-V)_{perceived}$. Quantitatively, we can measure the colour of stars using the intrinsic colour index $(B-V)_0 = B_0 - V_0$. Then $B_{perceived}$ is related to B_0 via the absorption A_B

$$B_{perceived} = B_0 + A_B$$

and this absorption A_B can be quantified using the optical depth. After making the observation with the blue filter, we repeat it with the green filter. Then, we calculate the difference between the two:

$$\left.\begin{aligned} B_{perçu} &= B_0 + A_B \\ V_{perçu} &= V_0 + A_V \end{aligned}\right\} \text{ in magnitude}$$

$$\begin{aligned} \left(B-V\right)_{perçu} &= \left(B-V\right)_0 - \left(A_V - A_B\right) \quad \text{with } A_B > A_V \\ &= \left(B-V\right)_0 + \underbrace{E\left(B-V\right)}_{\text{colour excess}} \end{aligned}$$

So, when $(B-V) > (B-V)_0$ the dust causes the object to appear redder.

3.3 TIDAL FORCES AND THE EARTH-MOON DISTANCE

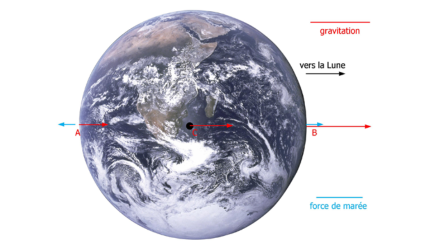

FIGURE 1

3:36 18:13

Principle of tidal forces.

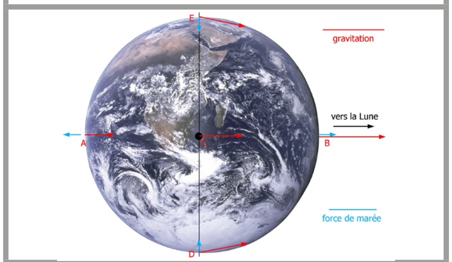

FIGURE 2

9:23 18:13

Principle of tidal forces.

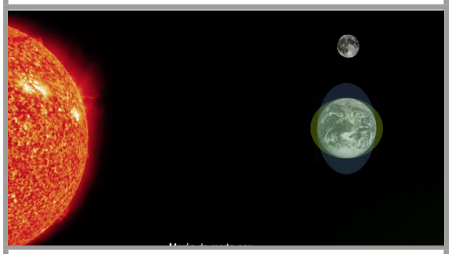

FIGURE 3

10:44 18:13

Neap tide.

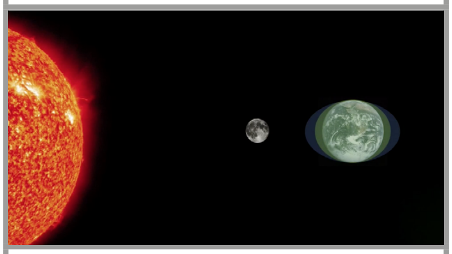

FIGURE 4

11:19 18:13

Spring tide.

On Earth, tidal forces result from the differential acceleration exerted by the Moon at ground level. The strength of the gravitation field of the Moon is not constant between the centre of the Earth and its surface.

As shown in figure 1, the Moon's gravitational field is stronger nearer the Moon. The Moon, therefore, attracts the right-hand side of the Earth with a certain force, and exerts a much smaller force on the other side. The magnitude of this force at the centre of the Earth is between these two values. The tidal force is calculated by subtracting the gravitational force at point C from the gravitational force at point A.

Assuming g_a for the acceleration due to gravity at point A, g_b is the acceleration due to gravity at point B, m is the mass of the Moon, d is the distance between Earth and Moon, and r is the radius of the Earth.

$$\begin{aligned} g_A - g_C &= \frac{Gm}{(d+r)^2} - \frac{Gm}{d^2} \\ &= \frac{Gm}{d^2}\left(1 - \frac{2r}{d}\right) - \frac{Gm}{d^2} \\ &= -\frac{2Gm}{d^3} r \end{aligned}$$

These difference between these acceleration values is called the tidal force. The fact that it is negative at point A means that it's pointing to the left, away from the Moon. Repeating the same calculations for point B:

$$\begin{aligned} g_A - g_C &= \frac{Gm}{(d-r)^2} - \frac{Gm}{d^2} \\ &= +\frac{2Gm}{d^3} r \end{aligned}$$

To determine the tidal forces at the poles, for example, we subtract the force vector at the centre of the Earth from the force vector at the pole. The horizontal components cancel, leaving only the vertical component. Thus, the Moon exerts a flattening effect on the Earth. The tidal forces exerted on the liquid part of the Earth's crust causes the oceans to stretch on either side of the Earth. Therefore, the high tides caused by the Moon track its position relative to the rotation of the Earth, always pointing both towards the Moon and away from it. The Sun also causes tidal forces. The magnitude of these forces is smaller, but they definitely exist.

Since the Moon orbits the Earth once every 28 days, whereas the Earth only orbits the Sun once every 365 days, the tides generated by the Moon change more quickly. The motion of the oceans in turn affects the rotation of the Earth. As they follow the path of the Moon, the oceans “rub” against the Earth’s crust, releasing energy that is ultimately lost into space. This phenomenon means that the Earth is losing energy and hence *angular momentum*, which causes the Earth’s rotation to slow, and the distance between the Earth and the Moon to increase. The Earth-Moon system is isolated, so its angular momentum is conserved. The friction between the oceans and the Earth’s crust causes the Earth to lose angular momentum, which is gained by the Moon. The distance between the Moon and the Earth increases by approx. 3.8 cm per year. The angular momentum of the Moon is $L = m\omega r^2$ where ω is the angular velocity and r is the Earth-Moon distance. Therefore, since $\dot{L} > 0$, $\dot{r} > 0$.

$$\begin{aligned} L &= m\omega r^2, \quad \dot{L} > 0 \\ L &= m(\dot{\omega} r^2 + 2\omega \dot{r} r) \quad \text{substituting the result on the right} \\ &= m\left(-\frac{3}{2}\omega \dot{r} r + 2\omega \dot{r} r\right) \\ &= \frac{1}{2} m\omega r\dot{r} \end{aligned}$$

BY KEPLER’S THIRD LAX, $\omega^2 r^3$ = CONSTANT. SO

$$\begin{aligned} \frac{d(\omega^2 r^3)}{dt} &= 2\dot{\omega}\omega r^3 + 3\dot{r} r^2 \omega^2 \\ &= \omega r(2\dot{\omega} r^2 + 3\omega \dot{r} r) = 0, \quad \text{hence} \end{aligned}$$

$$(2\dot{\omega} r^2 + 3\omega \dot{r} r) = 0 \quad \Rightarrow \quad \dot{\omega} r^2 = -\frac{3}{2}\omega \dot{r} r$$

4.1 THE ROCHE LIMIT

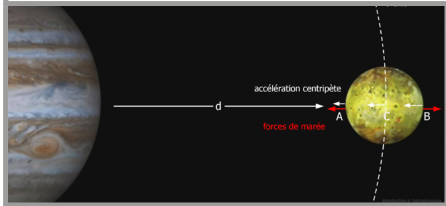

FIGURE 1

3:20 12:14

The Roche limit: the radius and the density of the planet are given by R and ρ_M. The radius and density of the satellite are r and ρ_m.

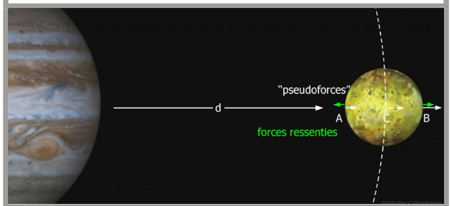

FIGURE 2

5:28 12:14

The Roche limit: the radius and the density of the planet are given by R and ρ_M. The radius and density of the satellite are r and ρ_m.

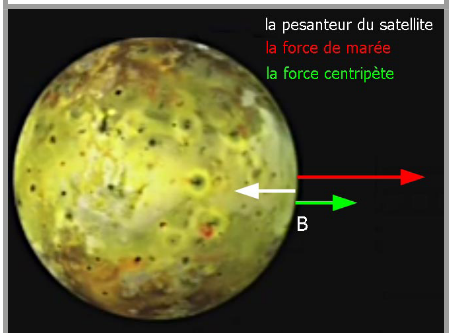

FIGURE 3

8:24 12:14

The Roche limit: the radius and the density of the planet are given by R and ρ_M. The radius and density of the satellite are r and ρ_m.

In extreme cases, tidal forces can deform celestial bodies to the point of causing them to break up. Some planetary rings, such as Saturn's rings, are thought to be the result of a satellite being torn apart under the effect of tidal forces. There is a limiting distance between two bodies before one of them is torn apart, called the "Roche limit" after the French astronomer Edouard Roche, who calculated it for the first time in the 19th century.

Neglecting the rotation of the satellite around the planet, the tidal force caused by the mass M at points A and B is given by

$$a_M(B) = \frac{2GM}{d^3} r$$

Assuming that the orbit has angular velocity $\omega = 2\pi/P$, we must add a centripetal acceleration $a = \omega^2 d$ where d is the distance between the centre of the planet and the centre of the satellite. This centripetal acceleration acts on the surface of the planet as a function of its distance from the centre of the planet in such a way that the acceleration is $a_A = \omega(d-r)$ at point A, $a_C = \omega^d$ at point C, and $a_C = \omega^2(d+r)$ at point B.

As a result of the centripetal acceleration towards the planet, a "pseudo-force" is experienced on its surface, with a magnitude equal to the centripetal force but acting in the opposite direction. To find the differential acceleration experienced by point A or B, we subtract the pseudo-force experienced at point C. The pseudo-forces thus experienced reduce to

$$\begin{aligned} a(B) &= \omega^2(d_r) - \omega^2 d \\ &= \omega^2 r \end{aligned}$$

We also know from Kepler's third law that

$$\frac{d^3}{P^2} = \frac{GM}{4\pi^2}, \quad \omega = \frac{2\pi}{P} \quad \Rightarrow$$

$$\omega^2 = \frac{GM}{d^3} \quad \text{so}$$

$$a(B) = \frac{GM}{d^3} r \quad \text{recall that the acceleration due to the tidal force is}$$

$$a(B)_{\text{tidal}} = 2\frac{GM}{d^3} r$$

There is therefore another differential acceleration due to the rotation of the satellite around the planet, equal to half of the tidal force. This adds to the effect of the tidal force. When the sum of the forces due to the rotation of the satellite and the tidal forces exceed the gravitational force of the satellite, the satellite begins to break up!

$$\begin{aligned} \left\| a_{\text{tidal}} + a_{\text{pseudo}} \right\| &> \left\| g \right\| \\ \frac{3GM}{d^3} r &> \frac{Gm}{r^2} \\ d &= \left(\frac{3M}{m} \right)^{1/3} r \end{aligned}$$

The distance below which the satellite begins to break up also depends on the density of both bodies. This means that, for $\rho = constante$:

$$m = \frac{4}{3}\pi r^3 \rho_m$$

$$M = \frac{4}{3}\pi r^3 \rho_M, \quad \text{substituting in the following equation}$$

$$d_{\text{Roche}} = 1.4\left(\frac{\rho_M}{\rho_m}\right)^{1/3} R$$

This approximation does not take into account the cohesive forces of the planet. The exact calculation gives

$$d_{\text{Roche}} = 2.5\left(\frac{\rho_M}{\rho_m}\right)^{1/3} R$$

If the distance is smaller than this, the satellite breaks up under the combined effect of the tidal forces and the centripetal force exerted upon it by its planet. In the solar system, the bodies most strongly affected by the Roche limit are probably the comets. They traverse the solar system at high speeds, often through strong gravitational fields that can cause them to break up if they pass closer than the Roche limit. This is precisely what happened to the comet Shoemaker-Levy 9 in May 1994 as it passed near Jupiter. The comet broke up into 21 pieces over a distance of roughly 1 million kilometres. Three months later, this debris returned to Jupiter and ultimately crashed into it on July 16th 1994, creating multiple points of impact that were visible for several days, and some of which were as large as the Earth.

4.2 COMETS

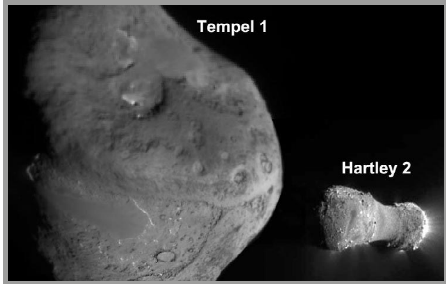

FIGURE 1
1:44 13:43

Cometary nuclei with diameters of 7.6 km and 2.2 km (image: NASA/JPL-Caltech/UMD).

FIGURE 2
2:08 13:43

Haley's comet (image: E. Kolmhofer, H. Raab; Joanes-Kepler-Observatory, Linz, Austria).

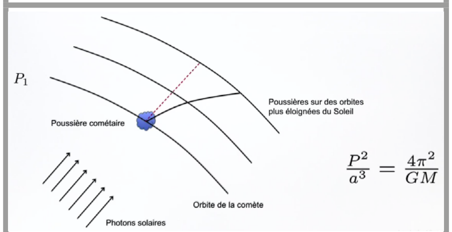

FIGURE 3
2:28 13:43

Illustration of solar photons "pushing away" comet particles by radiation pressure.

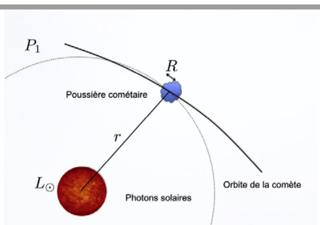

FIGURE 4
6:43 13:43

Illustration of solar photons "pushing away" comet particles by radiation pressure.

Comets are at most a few kilometres in diameter. They are composed of 80% ice and organic compounds such as carbon, hydrogen, oxygen, and nitrogen. Comets originate from a vast spherical cloud at the edge of the solar system called the Oort Cloud. The spherical geometry of this cloud and its estimated size of roughly 100,000 astronomical units were deduced from the fact that cometary orbits are occasionally highly eccentric and extremely elongated. Comets can have extremely large orbital periods ranging up to several centuries. Haley's comet, for example, has a period of 76 years. Their orbital inclinations are nearly random, so they arrive from almost every direction, completely at random. Small gravitational perturbations caused by other stars in the Milky Way can sometimes disrupt a comet, causing it to hurtle towards the Sun. The Oort Cloud is therefore a sort of natural reservoir of comets that formed at the same time as the solar system. As they approach the Sun, the surface of the nucleus of the comet melts, and matter is ejected in the form of a wide, diffuse tail. Figure 2 shows an ionized gas tail, as well a secondary, more diffuse tail composed of dust.

To see how these cometary tails are formed, consider a particle on the surface of a comet orbiting the Sun at a certain distance with period P^1. When the comet passes near the Sun, there are two competing forces: gravity acts on the particle, but so does the solar radiation pressure. The radiation pressure due to the flux of solar photons over a certain cross section is therefore in competition with the gravitational force, which also depends on the size of the particle, as a function of its density. The radiation pressure is proportional to R^2, the cross section of the particle, and the mass is proportional to R^3, where R is the radius of the particle. Therefore, whenever the radiation pressure exceeds the gravitational force, the particle is ejected from the comet's surface in the radial direction away from the sun, changing the orbit.

Kepler's third law states that the orbital period increases with the radius of the orbit. This give rises to a curved cometary tail.

The radiation pressure force is given by $F_{rad} = \frac{E}{c}\sigma_g$, where $E = h\nu = pc$ is the energy of a photon and σ_g is the cross section of the particle. The following forces are therefore involved:

$$
\begin{aligned}
F_{rad} &= \frac{E}{c}\sigma_g \quad \text{where} \quad E = \frac{L_0}{4\pi r^2}, \quad \sigma_g = \pi R^2 \\
&= \frac{L_0}{4\pi r^2 c}\pi R^2 \\
F_{grav} &= G\frac{M_\odot m_g}{r^2} \quad \text{where } m_g \text{ is the mass of the particle} \\
&= G\frac{M_\odot}{r^2}\rho_g \cdot \frac{4}{3}\pi R^3
\end{aligned}
$$

From this, we can derive the relationship between the gravitational force and the modulus of the radiation pressure.

$$\frac{F_{grav}}{F_{rad}} = \frac{16\pi G M_{\odot} R \rho_g c}{3L_{\odot}}$$

Based on this, we can calculate the particle radius at which these forces are in equilibrium, i.e. when $F_{grav}/F_{rad} = 1$. This radius is approximately 2,000 **Å**. As shown above, the mass of the particle is proportional to R^3 and the cross section is proportional to R^2. Therefore, above a certain radius (~2000 **Å**), the particle does not detach from the surface of the comet, but remains stuck to it.

In figure 2, in blue on the left, we can see a tail of ions, extremely small and light particles that are propelled directly out of the comet's orbit by the solar photons. On the left, we see a white tail of much heavier particles, which pick up momentum from the solar photons. This transfer of energy modifies the orbit of each particle. Outside the comet's orbit, the particles are slower than the comet, in agreement with Kepler's third law, which creates a curved tail.

4.3 THE ENERGY BALANCE OF PLANETS

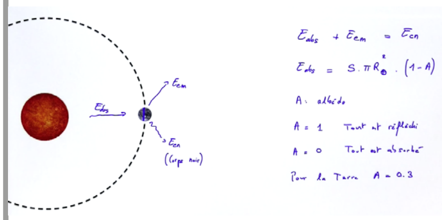

FIGURE 1

5:32 15:01

Energy balance of the Earth.

The energy balance of a planet is the balance between the received and emitted energy, and fully determines the physical condition at its surface. Consider, for instance, the energy received by the Earth. The Earth receives an energy flux from the Sun in the form of a force, called the solar constant. This flux is in the order of $S_\oplus = 1.37\times10^6\ \mathrm{erg\cdot s^{-1}\cdot cm^{-2}}$. This energy solar can be expressed as a function of the distance from the Sun by

$$S(d) = S_\oplus 4\pi d_\oplus^2 \cdot \frac{1}{4\pi d^2} = S\left(\frac{d_\oplus}{d}\right)^2$$

where $d_\oplus$ is the Earth-Sun distance in astronomical units and d is also measured in astronomical units.

In terms of outgoing energy, a certain amount of energy is emitted by the planet due to radioactivity in the Earth's mantle. Energy is also emitted in the form of black-body radiation. The absorbed energy (E_{abs}), the emitted energy (E_{em}), and the black-body energy (E_{bb}) are related by

$$E_{abs} + E_{em} = E_{bb}$$

The absorbed energy can be expressed as the solar constant times the cross section of the Earth. The fact that some energy is reflected is expressed by $(1 - A)$ where A is the *albedo* , a measurement of the reflectivity of a surface, equal to the ratio of the reflected luminous energy to the incident luminous energy.

$$E_{abs} = S\cdot\pi R_\oplus^2\cdot(1-A)$$

In the case of the Earth A=0.3, this means that 70% of the solar energy is absorbed.

If the radiation emitted by the radioactivity from molten magma beneath the Earth's crust is given by Q, the energy produced by this radioactivity at ground level, times the surface of the Earth is:

$$E_{em} = 4\pi R_\oplus^2\cdot Q$$

For the Earth this is $Q = 0.06\ \mathrm{W\cdot m^{-2}}$ at ground level. Finally, the energy emitted in the form of black-body radiation is given by

$$E_{bb} = \sigma T_{eff}^4 \cdot 4\pi R_\oplus^2$$

where T_{eff} is the effective temperature.

We can therefore rearrange the equation $E_{abs} + E_{em} = E_{bb}$ as follows

$$1 + \frac{4Q}{(1-A)S} = \frac{4\sigma T_{eff}^4}{(1-A)S}$$

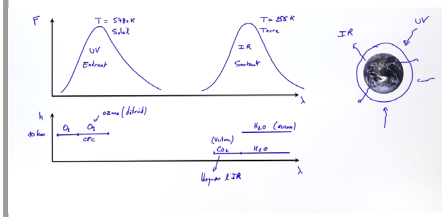

FIGURE 2

13:48 15:01

Energy balance for the Earth: effect of the chemical composition of the atmosphere on the incoming and outgoing radiation.

The numbers on the right allow us to deduce that the effective temperature of the Earth as a black body is $T_{eff} = 255\ °\mathrm{K}$, in the infrared band.

For the Earth:

$$A = 0.3$$
$$Q = 0.06\ \mathrm{W \cdot m^{-2}}$$
$$S_{\oplus} = 1.37 \cdot 10^{6}\ \mathrm{erg \cdot s^{-1} \cdot cm^{-2}}$$

The atmosphere acts as a filter, so that there is an incoming radiation peak at 5,780°K in the ultraviolet from the Sun, whereas the outgoing radiation peak leaving the atmosphere is 255°K in the infrared band. This filter consists of several layers. Different molecules are present at different heights and absorb different wavelengths of radiation. O_2 and O_3 (ozone) are found at 10-12 km. They absorb almost all wavelengths below 300 nanometres, i.e. ultraviolet radiation. Water (H_2O) can also be found relatively high in the atmosphere, created by kerosene combustion in aircraft engines closer to the ground. It absorbs most wavelengths above 700 nm. After combining the absorption spectra of the various gases in the atmosphere, there are low-opacity "windows" that allow certain bands of light through. The optical window ranges from around 300 nm (ultraviolet-C) to wavelengths that can be perceived by humans in the form of visible light at around 400-700 nm and continues to around 1,100 nm in the infrared region. There are also atmospheric windows for radio waves that allow higher wavelengths through.

Changes in the atmosphere during modern times include the destruction of the ozone layer by CFCs (chlorofluorocarbons), which allows UV radiation to reach the ground, increasing the heating effect experienced by the Earth. An additional layer of water has also been created, as well as CO_2 created by the combustion of hydrocarbons, which blocks outgoing infrared radiation. More energy is therefore retained at ground level. Without human intervention, a natural equilibrium usually developed between the incoming and outgoing filters. This equilibrium can, however, be broken by adding water filters and CO_2, or by destroying the ozone filters that partially block ultraviolet radiation.

4.4 PLANETARY ATMOSPHERE

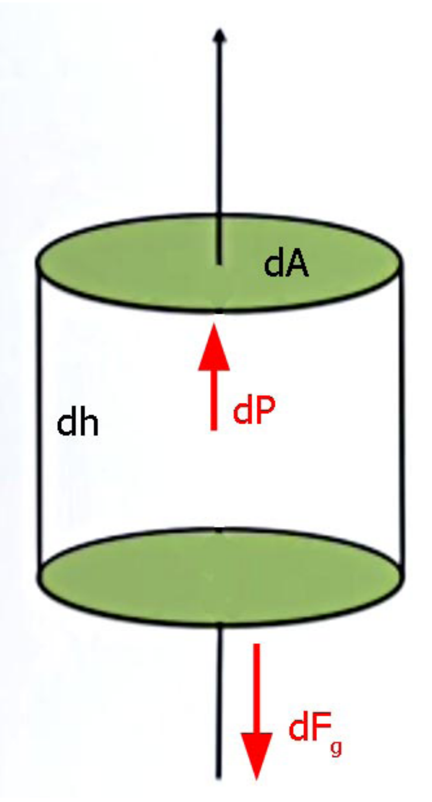

FIGURE 1

1:23 13:10

The volume element is located at a certain altitude h. It has surface area dA, height dh and density ρ.

EQUATION OF HYDROSTATIC EQUILIBRIUM

The equation of hydrostatic equilibrium allows us to determine the characteristics of a planet's atmosphere. As the name suggests, it describes a state of equilibrium between gas pressure, which acts upwards, and gravitational force, which acts downwards. In figure 1, these two forces are shown acting on a volume element, a column of atmosphere. Since there is equilibrium, the pressure force within the volume element is equal to gravity:

$$\begin{aligned} dP\,dA &= -dF_g \\ &= -gdm = -g\rho\,dV, \quad \rho = f(h), \quad g = f(h) \\ &= -\rho(h)g(h)dA\,dh \quad \Rightarrow \\ \frac{dP}{dh} &= -\rho(h)g(h)dA \end{aligned}$$

Depending on the conditions in which this equation is used we can very often simplify it by assuming that $\rho = constante$. In the case of a large planet with a relatively thin atmosphere, g varies very little in the atmosphere:

$$\frac{dP}{dh} = -\rho g$$

To solve this equation, we can make use of the Boltzmann equation

$$P = nkT$$

where T is the temperature, k is the Boltzmann constant, and n is the numerical density of the particles, with

$$n = \frac{\rho}{\bar{\mu}\cdot m_\mu}$$

where $\bar{\mu}$ is the average molecular mass and $m_\mu = 1.66\times10^{-27}$ kg is the atomic mass unit. Therefore, from the ideal gas equation, we can derive an expression for ρ that can be substituted into the equation $dP/dh = -\rho g$ above

$$\begin{aligned} \frac{dP}{dh} &= -\rho g, \quad \rho = \frac{P\mu m_\mu}{kT} \\ &= -g\frac{P\bar{\mu}m_\mu}{kT} \quad \Rightarrow \\ \frac{dP}{dt} &= -\frac{g\bar{\mu}m_\mu}{kT}\cdot dh, \quad H = \frac{kT}{g\bar{\mu}m_\mu} \\ \frac{dP}{P} &= -\frac{1}{H}dh \quad \text{by integrating} \\ \mathrm{P} &= ke^{\frac{h}{H}} = P_0e^{\frac{h}{H}} \end{aligned}$$

where H is the characteristic depth of the atmosphere and P_0 is the air pressure at ground level. The pressure profile is therefore exponential with respect to the altitude.

AVERAGE MOLECULAR MASS μ

To calculate the average molecular mass, we begin by counting the average number of particles (nucleons) in the atmosphere. The atmosphere consists of approximately 78% molecular nitrogen (N_2) and 22% molecular oxygen (O_2). Nitrogen has 7 protons and 7 neutrons per atom, so there are 28 nucleons per molecule of nitrogen. Molecular oxygen has 32 nucleons. The average mass of the molecules in the atmosphere is therefore

$$\bar{\mu} = \frac{(0.78 \times 28) + (0.22 \times 32)}{0.78 + 0.22} = 29 \text{ u (atomic mass units)}$$

CONDITION FOR RETAINING AN ATMOSPHERE

To determine whether a given planet can retain its atmosphere, we need to compare the escape velocity of a molecule in the atmosphere with its most probable velocity. The escape velocity is found by equating the kinetic energy of the particle with its potential energy:

$$\frac{1}{2} m v_e^2 = mgR$$

$$v_e = \sqrt{2gR}$$

where R is the radius of the planet. The most probable velocity is given by

$$\bar{v}_m = \sqrt{\frac{2kT}{\bar{\mu} m_\mu}} = \sqrt{2gH}$$

by comparing the two terms v_e and $\bar{v}_m$, we see that a planet can retain its atmosphere whenever $R > H$.

	VENUS	EARTH	MARS
THE SOLAR CONSTANT (kW · m^{-2})	2.6	1.4	0.6
ALBEDO	0.7	0.3	0.2
BLACK-BODY TEMP. (°K)	230	255	216
GROUND TEMP. (°K)	735	288	210
P_0: PRESSURE AT GROUND LEVEL (BAR = ATM.)	93	1	6 x 10-3
H: CHARACTERISTIC HEIGHT (KM)	14	8	11
R : RADIUS OF THE PLANET (KM)	6,052	6,371	3,390

Summary of key atmospheric and temperature properties of the terrestrial planets.

5.1 STAR FORMATION

THE JEANS' LENGTH AND THE JEANS' MASS

Stars form in groups from a gas cloud that fragments due to its inherent inhomogeneities. If the pieces arising from this process have more than a certain mass or a certain radius, known as the Jeans' mass and the Jeans' length, they contract and become hotter until hydrogen fusion reactions are triggered, giving birth to a star. This process can be explained in terms of the virial theorem. For a nebula with density ρ, mass M, N particles and with radius R :

$$\begin{aligned}\langle K\rangle &= -\frac{1}{2}\langle U\rangle, \quad \langle K\rangle = \frac{3}{2}NkT, \quad \langle U\rangle = -\frac{3}{5}\frac{GM^2}{R}\\ 3NkT &= \frac{3}{5}\frac{GM^2}{R}\end{aligned}$$

But if there is insufficient kinetic energy relative to the potential energy, the gas cloud will begin to collapse.

$$\text{if}\left\{\begin{aligned}\langle K\rangle &< -\frac{1}{2}\langle U\rangle\\ 3NkT &< \frac{3}{5}\frac{GM^2}{R}\\ kT &< \frac{G\bar{m}}{5R}M, \quad \bar{m} = \frac{M}{N}\\ kT &< \frac{G\bar{m}}{R}\frac{4}{3}\pi R^3\rho, \quad M = \frac{4}{3}\pi R^3\rho\\ \sqrt{\frac{15kT}{4\pi G\bar{m}\rho}} &< R, \quad \bar{m} = \bar{\mu}m_\mu\end{aligned}\right\}\text{the star collapses}$$

The Jeans' radius is the minimum radius above which the nebula cloud collapses:

$$\begin{aligned}R_{Jeans} &= \sqrt{\frac{15kT}{4\pi G\bar{m}\rho}}\\ M_{Jeans} &= \frac{4}{3}\pi\rho R^3_{Jeans}\end{aligned}$$

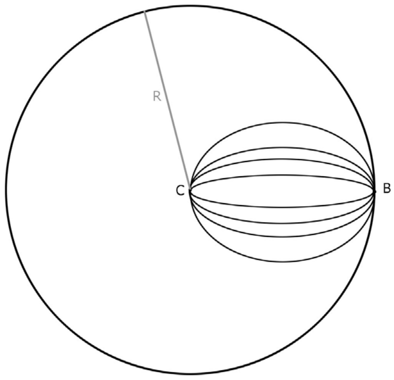

FIGURE 1

7:28 13:39

Significance of free-fall time.

FREE-FALL TIME

The free-fall time is the time that the cloud requires to collapse into a single central point. It is very difficult to calculate. Consider a nebula cloud of radius R whose particles are initially positioned at the edge of the cloud B and which move towards the centre C. We can view this straight line as an ellipse with infinite eccentricity, so that the particles can reach the centre via any "orbital" route from B to C. The time required to reach the centre is therefore equal to half of one of these orbits. This period does not depend on the eccentricity. We therefore have

$$t_{ff} = \frac{P}{2} \quad \text{and by Kepler's laws}$$

$$P^2 = \frac{4\pi}{GM^2}\left(\frac{R}{2}\right)^3 \quad \text{the semi-major axis is R/2}$$

$$= \frac{3\pi}{8G\rho} \Rightarrow$$

$$t_{ff} = \sqrt{\frac{3\pi}{32G\rho}}$$

t_{ff} only depends on ρ.

According to the table below, given the density of the Sun, it would require half an hour to collapse. The reason that this does not happen is related to the energy balance of the Sun. The virial theorem tells us that half of the potential energy lost by the Sun in the form of luminosity is converted into kinetic energy. This system of equations has the solution

$$\left.\begin{aligned} dE_{tot} &= dU + dK = -Ldt \\ dU + 2dK &= 0 \end{aligned}\right\} \Rightarrow \begin{cases} dU = -2Ldt \\ dK = +Ldt \end{cases}$$

	DENSITÉ (kg · m^{-3})	t_{ff}
UNIVERSE	10^{-27}	10^{-11} years
GALAXY	10^{-21}	10^{8} years
INTERSTELLAR MEDIUM	$10^{-21}/10^{-27}$	$10^{5}/10^{8}$ years
SOLAR SYSTEM	10^{-27}	1,000 years
SUN	1,400	1,800 years

Free-fall time of bodies with different average densities.

The star loses potential energy as radiation in the form of luminosity. However, half of the lost potential energy is converted into kinetic energy. This energy is transformed into heat, which in turn emits photons as black-body radiation or by ionization. These emissions create a radiation pressure on the outer layers of the star, which are in the process of collapsing. This effect counteracts gravity and prevents the star from collapsing.

THE LIFETIME OF A STAR

The lifetime of a star (the Helmholtz-Kelvin time scale) is the time required for a star to lose half of its potential energy to radiation. This depends on the luminosity of the star.

$$L \cdot t_{HK} = \frac{U}{2}$$

$$t_{HK} = \frac{U}{2L} = \frac{3}{10}\frac{GM^2}{RL}$$

The lifetime of the sun is ~ 500 years.

Stars draw energy from both gravitational contraction and nuclear reactions.

5.2 STELLAR CLASSIFICATION/HR DIAGRAM

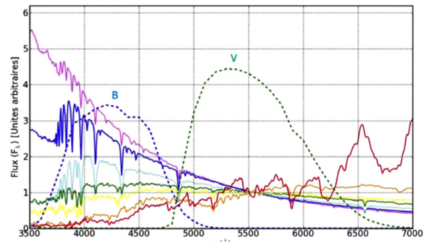

FIGURE 1

2:16 21:46

Examples of stellar spectra in the optical range.

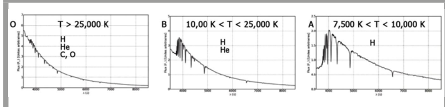

FIGURE 2

5:50 21:46

Harvard classification: O, B, A.

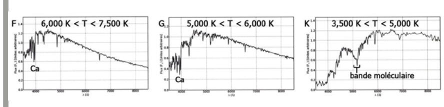

FIGURE 3

8:52 21:46

Harvard classification: F, G, K and M.

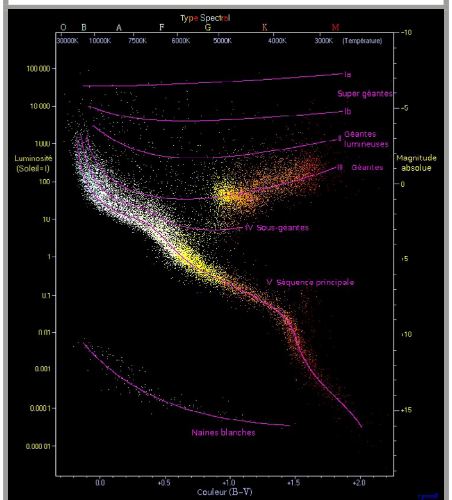

FIGURE 4

13:42 21:46

Hertzsprung-Russell diagram of the Milky Way.

We can classify stars according to their luminosity and their colour or, in other words, as a function of their black-body temperature.

SPECTRAL CLASSIFICATION

Figure 1 shows the seven known types of star, classified according to their black-body temperature. We see that one type has peak flux in the ultraviolet band, which corresponds to a relatively short wavelength. Others have peak flux in the infrared band, i.e. a relatively long wavelength. The Sun is in between, with peak flux in the yellow region.

To measure the colour of stars, we calculate the colour indices, usually by using B and V filters in the optical band. We then measure the slope of the spectrum as a function of the colour index, i.e. the slope of the line between the value of the flux at the centre of the bandwidth of filter B and its value at the centre of the bandwidth of filter V. The resulting slope is the B-V index, which is an indicator of the spectral type of the star. If the B-V index is large, the star is red. But if the B-V index is negative, the star is bluer.

The spectral classification, known as the Harvard classification, is based on these spectra. There are seven spectral classes: O, B, A, F, G, K and M in order of decreasing temperature. Each spectral type has its own lines. Hydrogen is present in each case but its spectral lines can be stronger or weaker depending on the temperature. Very hot stars also have helium lines. If the star is extremely hot, there can also be lines with much higher ionization potential, such as carbon or oxygen.

At high temperatures, molecules are destroyed. But at lower temperatures (K class), the molecules remain intact, producing broad absorption lines that actually consist of a large number of very thin lines that are inseparable at the resolution of our instruments. These are called molecular bands.

There are 7 spectral classes: O, B, A, F, G, K, M; and 10 subclasses labelled 0-9. There are also 7 luminosity classes: Ia, Ib, II etc. VI. For example, the Sun is a type G2V star: G indicates the temperature, 2 is from a scale that divides the temperature into 10 smaller intervals and V is the luminosity class of the Sun, which happens to be shared by 80% of all stars.

Colour-magnitude diagrams, or Hertzsprung-Russell diagrams, can be used to sort the stars in a star cluster according to their luminosity on the vertical axis and their black-body temperature/colour on the horizontal axis. The Hertzsprung-Russel diagram of 22,000 stars in our Milky Way (fig. 4) has four axes: at the top, the spectral classes: O, B, A, F, G, K and M; at the bottom, the B-V colour index. On the left the luminosity and on the right the absolute magnitude, which increases in the downwards direction. Around 80% of all stars are located in the main sequence, and will burn hydrogen into helium for the duration of their lifetimes.

THE ISO-RADIUS LINE

Take the logarithm of the luminosity written in solar units

$$L = 4\pi R^2 \cdot \sigma T^4$$

$$\frac{L}{L_\odot} = \left(\frac{R}{R_\odot}\right)^2 \left(\frac{T}{T_\odot}\right)^4$$

$$\log L = 2\log R + 4\log T$$

If R is fixed, this becomes the a straight line on a log-log scale, a straight line of type $y = ax + b$. This provides a method of normalizing the radii so that we can compare the luminosity as a function of the temperature.

THE INTERSTELLAR ABSORPTION EFFECT

Interstellar absorption is the result of dust clouds and other objects between the observer and the observed star. This effect influences the colour-magnitude diagram. The intrinsic magnitude of an object is equal to its observed magnitude plus absorption (which weakens it) $m=m0+A$ where A is the colour-dependent absorption coefficient. The interstellar absorption effect not only reduces the magnitude, but also causes the colour to shift towards red. Therefore, absorption induces a downward shift on the Hirschsprung-Russell diagram due to the dimmed luminosity, as well as a rightward shift due to redshift. We must therefore be careful when making conclusions based on stellar populations in colour-magnitude diagrams, since they may be affected by absorption along the line of sight of the star that is being observed.

STAR SIZE

The radius of a star is not a directly observable quantity. Write f for the flux received on Earth at a distance d from a star of radius R and F for the flux at the surface of this same star. These relationship between these two values is

$$\begin{aligned} f &= F \cdot 4\pi R^2 \cdot \frac{1}{4\pi d^2} \\ &= F\left(\frac{R}{d}\right)^2, \quad \alpha = \frac{R}{d} \\ &= F\alpha^2 \end{aligned}$$

This α is simply the angular radius of the star, i.e. the radius subtended by the star at certain distance. The observed flux depends on the distance and the size (radius) of the star. A hypergiant at a distance of 200 parsecs, i.e. a very close star, would have a radius of 1,000 times the solar radius, which gives $\alpha \approx 0.02$ arcseconds, which is roughly two times smaller than the smallest details currently observable through a telescope. The Sun is therefore the only star whose surface we can see in detail.

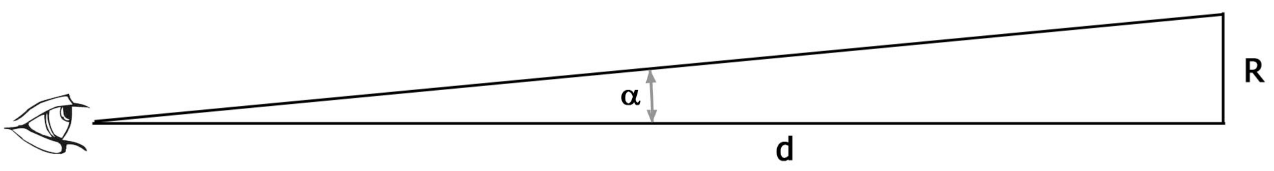

FIGURE 5

20:25 21:46

Physical size (R) and angular size (α) of stars.

5.3 STELLAR EVOLUTION: THE LIFE AND DEATH OF STARS

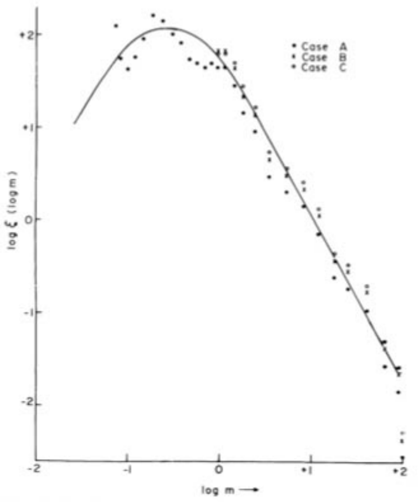

FIGURE 1

2:18 22:11

Initial mass function.

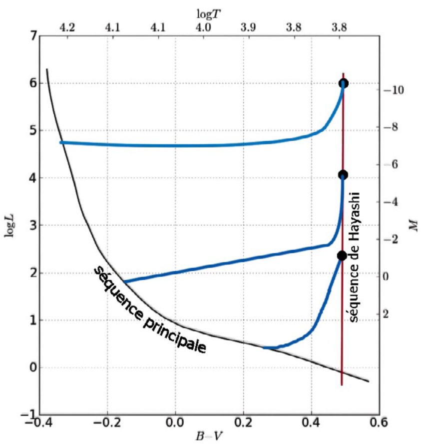

FIGURE 2

6:30 22:11

The Hayashi track, shown in red.

BIRTH: THE HAYASHI TRACK

Stars are born from the fragmentation of gas and dust clouds and the contraction of the resulting clusters. The initial clouds have a certain mass distribution that we can represent on a log-log scale, called the *initial mass function*. The initial mass function specifies the distribution of the nebula fragments in solar mass units relative to the log of the number of fragments. If we plot these clouds on a magnitude-colour diagram as they fragment, giving birth to stars, we find a nearly vertical isothermal sequence along the luminosity axis. This sequence is called the *Hayashi track*. It consists of several proto-stars of various sizes (fig. 1), but which all have the same temperature. At this stage, the material in the protostars is mixed together as the star begins to contract. There are not yet any nuclear reactions taking place.

Gradually, as the radius of the protostar decreases, the temperature in the centre increases until a nuclear reaction is triggered. This reaction immediately counteracts the contraction, in two different ways: by radiation pressure and by gas pressure from the turbulent motion due to internal heat. Additionally, as the protostar contracts, it becomes increasingly opaque, which reduces its luminosity. According to the equation

$$L = 4\pi R^2 \sigma T^4$$

The essentially constant decrease of L with T causes R to decrease.

Although the temperature remains constant in the outer regions, it increases at the centre, until nuclear reactions are triggered. When these reactions begin to occur, the temperature of the star rises very quickly until it reaches a position on the main sequence, passing through the blue steps shown in figure 2. The higher the mass of the star, the faster these nuclear reactions are ignited. Therefore, stars with lower mass travel more slowly down the Hayashi track before migrating to the main sequence.

Once they have joined the main sequence, stars burn their hydrogen by means of nuclear fusion reactions that transform hydrogen nuclei into helium nuclei $4H \Rightarrow {}^4He$. This fusion can occur in two different ways in either a complex chain of reactions or a simpler chain. The boundary between the two possible types of reactions is at 1.3 times the solar mass.

LEARN FASTER, LEARN BETTER!

BOOCs EPFL

Introduction to Astrophysics
Frédéric Courbin

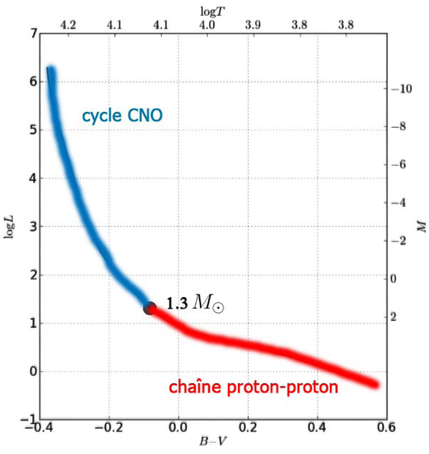

FIGURE 3

7:46 22:11

The two hydrogen-to-helium fusion paths in stars with different masses on the main sequence.

THE ×1.3 THRESHOLD $M_\odot$

Above 1.3 times the solar mass, stars burn hydrogen into helium according to what is known as the CNO cycle. Below this threshold there is the proton-proton chain reaction. In fact, despite what its name seems to suggest, the CNO cycle produces neither carbon, nor nitrogen, nor oxygen. The proton-proton chain does involve protons, but both reactions result in the fusion of four hydrogen nuclei into one helium nucleus. This mass limit also corresponds to a temperature limit. The CNO reaction requires higher temperatures. The most important thing to remember is that stars on the main sequence burn hydrogen into helium throughout most of their lifetime.

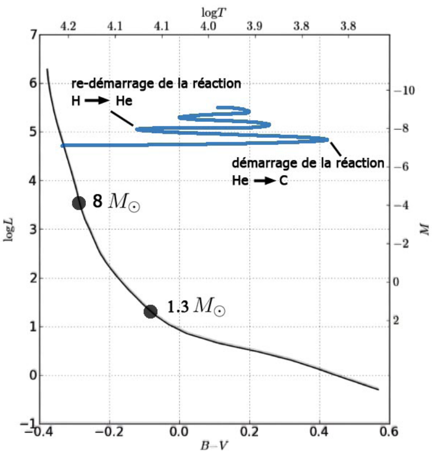

FIGURE 4

12:05 22:11

Path of a star with high mass on the HR diagram over the course of its death.

THE 8× THRESHOLD $M_\odot$

On the main sequence, there is an equilibrium between the gas pressure and the radiation pressure on the one hand, and gravity on the other. At 8 times the solar mass, there is another threshold that determines the way that the star will die. For stars with more than 8 times the solar mass, once hydrogen fusion stops, the gas pressure and the radiation pressure decrease, allowing gravity to dominate. Two phenomena occur: 1) *the outer regions of the star cool down* and 2) even though the core of the star contracts, the outer layers expand, causing the radius of the star to grow. This outer cooling causes the star to become redder. At the same time, *the inner warming* triggers another kind of nuclear reaction, transforming helium into carbon.

As the radius of the star increases and the temperature decreases, the star shifts to the right on the colour-magnitude diagram, towards lower temperatures and redder surface colour regions. Eventually, for stars with very high masses, the core contracts, and the reaction transforming helium into carbon is triggered. When this happens, the star naturally begins to heat up, moving further to the left on the HR diagram. A sequence of nuclear reactions occurs between these two alternatives, each reaction shorter than the last, until the iron fusion reaction is ultimately triggered. This reaction is endothermic. It produces neither photons nor outward radiation pressure, but it absorbs energy. The star then collapses fully on itself, becoming a supernova. If the star originally had an extremely high mass, a black hole or a neutron star can potentially form after the supernova explosion.

Something similar occurs for stars with mass smaller than 8 times the solar mass. They can develop into giant stars, which cool until they settle in a certain position on the colour-magnitude diagram, while becoming redder. The outer layers swell while the core contracts, until the nuclear reaction $He \Rightarrow C$ is triggered, but there is no iron fusion reaction. After moving back and forth a few times across the HR diagram, the core contracts until it can no longer ignite the next nuclear reaction. The star then dies, leaving behind its outer layers, which become a planetary nebula centred on a dead star, a white dwarf, which shines only by the emission of stored thermal energy.

Some stars have even lower mass. Stars whose mass falls between $0.08\ M_\odot < M < 0.26\ M_\odot$ are white dwarfs that formed directly from a proto-stellar cloud. Stars with a mass below $0.08\ M_\odot$ are too small to ignite a nuclear reaction. These stars are known as brown dwarfs. These stars shine due to gravitational contraction only.

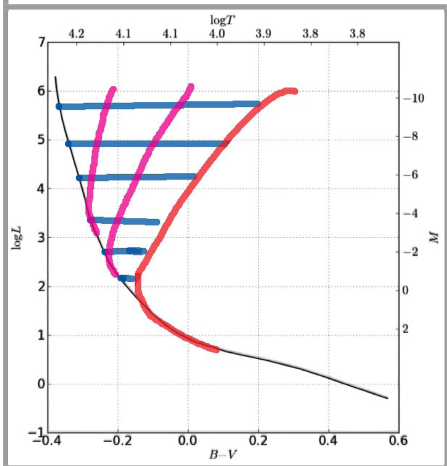

FIGURE 5
18:48 22:11

Determining the age of star clusters using the shape of the main sequence.

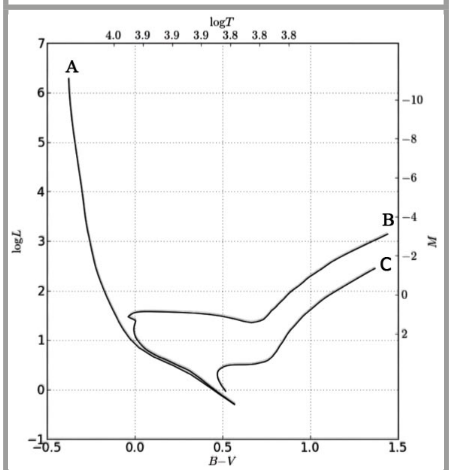

FIGURE 6
19:32 22:11

Isochrones of A=10^6 years, B=10^9 years and C= 10^{10} years.

THE AGE OF STAR CLUSTERS

We can use the colour-magnitude diagram to find the age of stellar populations. Stars on the main sequence burn hydrogen. The larger the mass of the star, the faster it burns its hydrogen. Larger stars therefore leave the main sequence earlier, since they are positioned higher up on the sequence. The higher the mass of the stars shown in figure 5, the further they are located towards the right of the graph. If we connect these stars with a line (in red), we obtain what is known as an *isochrone*, which connects together all stars of the same age. At the top of the curve in the isochrone, the stars have enough mass to leave the main sequence. Other isochrones (in pink) show younger stars.

The isochrone A in figure 6 shows the main sequence of very young stars with an age of around 10^6 years. Note that on the isochrone showing stars with an age of 10^9 years, there are no stars in the upper parts of the diagram, since all of these stars have disappeared. They were extremely massive, with more than 8 times the solar mass, and burned away all of their hydrogen, ultimately exploding. Some of the stars on the left are still on the main sequence and are still burning hydrogen, but the most massive stars have moved towards the branch of giant stars on the right. So now, the older clusters contain only low-mass stars that are still on the main sequence, since almost all of the other stars have moved towards the branch of giant stars. Therefore, the curve reflects the migration of stars over time, and we can determine the age of a cluster simply by looking at its position on the curve.

6.1 GALAXIES

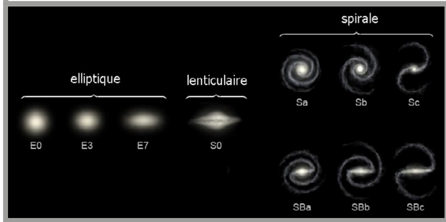

FIGURE 1

1:36 22:20

The Hubble sequence (image: Wikipedia).

HUBBLE'S "EVOLUTIONARY" SEQUENCE

In the Hubble sequence, there are two main categories of galaxies: elliptical galaxies and spiral galaxies. Between the two, there is an intermediate type of galaxies, called lenticular galaxies. Elliptical galaxies typically contain older stars with random orbits around a common centre of gravity. These galaxies are subdivided into 7 possible ellipticities E0-E7. The numerical designation is determined by the ratio of the major axis (a) to the minor axis (b).

Spiral galaxies are designated with an S followed by a, b, or c depending on the size of the central bulge relative to the spiral arms of the galaxy and the space between the arms. As shown in figure 1, as the designation increases from Sa to Sc, the galaxies have fewer spiral arms and these are wrapped less tightly around the bulge. Spiral galaxies also have halos of dark matter. Similarly, there are barred spiral galaxies whose arms are wrapped around a bar instead of a bulge. These are designated as SBa-SBc. Lenticular galaxies are somewhat similar to spiral galaxies with an enormous bulge the same size as those in an elliptical galaxy.

Hubble created this sequence under the assumption that galaxies are born with an elliptical shape, and gradually evolve spiral arms. But this isn't true. Therefore, this is a morphological sequence rather than an evolutionary sequence.

ELLIPTICAL GALAXIES

The most massive elliptical galaxies (between $10^7\ M_\odot$ et $10^{13}\ M_\odot$) are often but not always found at the centre of a galaxy cluster. Their stellar populations tend to be older, billions of years old. They consequently have relatively little gas and dust, and relatively low levels of stellar formation. The luminous flux emitted by an elliptical galaxy is given by

$$F = F_0 e^{-\left[\left(\frac{r}{r_e}\right)^{\frac{1}{4}} - 1\right]}$$

where F is a normalisation factor and *r* is the effective radius, containing half of the light generated by the galaxy. This light profile is known as a *de Vaucouleurs' profile*.

FIGURE 2
5:55 22:20
Messier 101, an Sab galaxy, in between Sa and Sb (image NASA/ESA-Hubble Heritage).

FIGURE 3
10:02 22:20
NGC 4565, a spiral galaxy, viewed from the side (image: ESO).

SPIRAL GALAXIES

The mass of spiral galaxies has a smaller range than that of elliptical galaxies, between $10^9\,M_\odot$ et $10^{12}\,M_\odot$. They have a diameter of approximately 40 kiloparsecs. This figure is relatively vague, since there is a halo of invisible dark matter around the bulges and spiral arms. Spiral galaxies also contain a lot of gas and dust, in which new stars are being born. Their stellar populations are composed of two components. The bulge contains older, low-mass stars, whose black-body radiation is reddish. The spiral arms, on the other hand, contain younger, more massive stars with bluer radiation.

The light profile of a spiral galaxy also has two components. The profile of the disc component is given by

$$F = F_0 e^{-\frac{r}{h}}$$

where *h* is the characteristic height of the disc. The second component, the light generated by the bulge, has a de Vaucouleurs profile, similar to elliptical galaxies.

FIGURE 4
11:48 22:20
Image of Messier 83, an Sab-type galaxy (image: NASA/ESA-W. Blair (John Hopkins)).

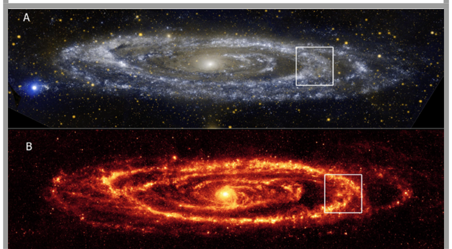

FIGURE 5
16:08 22:20
The Andromeda galaxy, viewed through ultraviolet (A) and infrared (B) filters (image: NASA/JPL/Caltech).

STELLAR POPULATIONS IN GALAXIES

The diagnostic tools available to us for studying galaxies in more detail include spectra and images. The image in figure 4 was taken with 3 filters, one blue, one of an intermediate colour, and one around the $H\alpha$ line. The $H\alpha$ filter shows the gas that has been ionized by hot stars as they were formed, as well as highly massive stars. These stars appear red because $H\alpha$ has a wavelength closer to the red band, whereas the black-body radiation of these stars is closer to blue. Young stars, in the process of being formed, appear blue. We can use filters like this together with the luminous flux to analyze a galaxy step by step, reconstructing the evolutionary history of its stellar population.

We can also use sets of filters whose wavelengths are further apart to analyze galaxies. In figure 5, in the white square, there is a spiral arm that is very visibly marked by a cluster of bright spots. The ultraviolet region shows massive, hot stars. These stars ionize the gas around them, emitting clusters of small spots in the $H\alpha$ line. On the other hand, in the infrared image, we see gas and dust heated by hot stars, causing it to re-emit black-body radiation the peak of which is located far into the infrared region. Both processes take place at the same location, but involve very different physical processes, and must be viewed with different types of tool in order to be seen.

We can use the Doppler effect to determine the radial velocity of the stars within the galaxy as a function of their position. By measuring the velocities away from us and the velocities towards us, we can calculate the mass of the galaxy using the laws of gravitation.

$$a = \frac{GM(r)}{r^2} = \frac{v^2}{r} \quad \Rightarrow$$
$$v = \sqrt{\frac{GM(r)}{r}}$$

This allows us to measure the mass inside this radius.

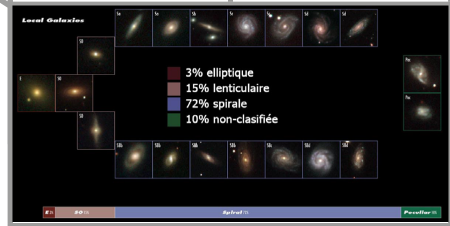

FIGURE 6

18:36 22:20

Morphological types as a function of distance, local universe (image: NASA/ESA–Sloan Digital Sky Survey, R. Delgado-Serrano and F. Hammer (Paris Observatory)).

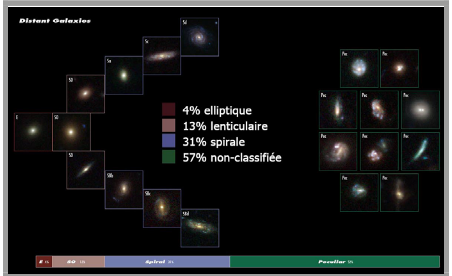

FIGURE 7

19:59 22:20

Morphological types as a function of distance, distant universe (image: NASA/ESA–Sloan Digital Sky Survey, R. Delgado-Serrano and F. Hammer (Paris Observatory)).

AGE AND DISTANCE

In fact, Hubble's morphological classification changes as a function of distance. This observation reflects the age of the regions being examined. Since the universe has been expanding since the Big Bang, by observing objects at various distances from us, we can see different periods in the life of the universe. Figure 6 shows a morphological classification that lists the proportion of each type of galaxy within the local universe. If we repeat this observation for more distant galaxies (fig. 7), the numbers are completely different, since these galaxies are at a different point in their lifetimes.

All of our theoretical ideas need to take into account the morphological classification of galaxies as a function of their distance, their masses as determined by measuring the Doppler effect, the rotational velocity of each galaxy, and the study of their stellar populations using colour-magnitude diagrams, which again depends on the distance.

6.2 GALAXIES: NUMERICAL ILLUSTRATIONS

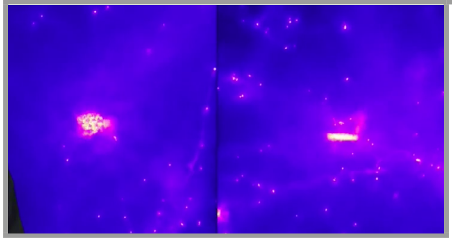

FIGURE 1

2:38 04:37

On the left, front view of the galaxy;
on the right, side view of the same galaxy
(simulation: Yves Revaz, EPFL).

FIGURE 2

3:13 04:37

Destruction of a galaxy by tidal forces.
One of the spiral galaxies, near the top,
is caught in the potential well highlighted by
the red circle (simulation: Yves Revaz, EPFL).

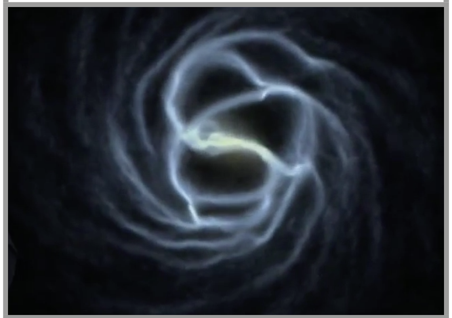

FIGURE 3

4:17 04:37

Gravitational instability within a galaxy
(simulation: Yves Revaz, EPFL).

In the early 20th century, Hubble thought that elliptical galaxies evolved into spiral galaxies over time according to his morphological sequence. We now know that spiral galaxies can actually become elliptical galaxies and vice versa. Collisions between galaxies have been discovered to play an important role, and the quantity and kinetic properties of dark matter are decisive factors in the creation and ultimate fate of each galaxy. If dark or luminous matter is dynamically cold, i.e. the lower the thermal agitation at the centre of a massive object, the more susceptible it is to collapsing in on itself, creating compact structures such as galaxies or clusters of galaxies.

Its motion can be simulated by allowing 33 million massive particles to interact within a region of space spanning 20 megaparsecs in each direction. The particles in the simulation only represent gas. Starting the simulation at age zero, the universe is almost homogeneous. However, the matter begins to collapse in on itself in the slightly denser regions, forming nodes and filaments. A spiral galaxy can be seen to form and briefly stabilize before being destroyed as it passes through a cluster of galaxies. This kind of simulation clearly illustrates the many possible paths that a galaxy can follow from its birth to its ultimate death.

6.3 ROTATION OF THE MILKY WAY

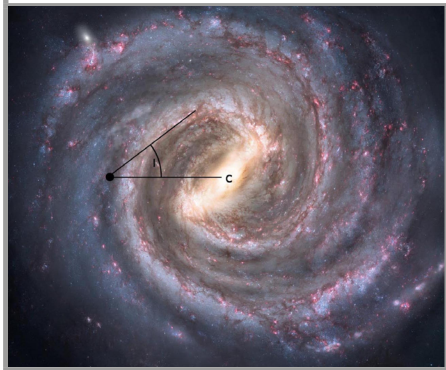

FIGURE 1

3:00 18:59

The spherical coordinate system of the Milky Way.

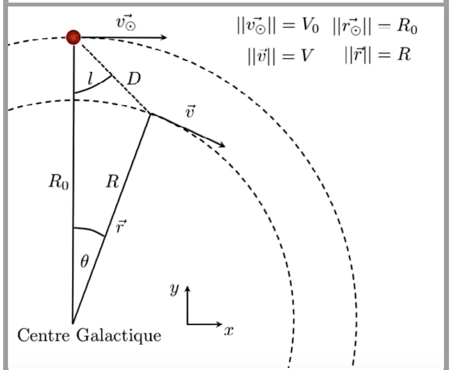

FIGURE 2

3:49 18:59

Motion of the Sun within the Milky Way.

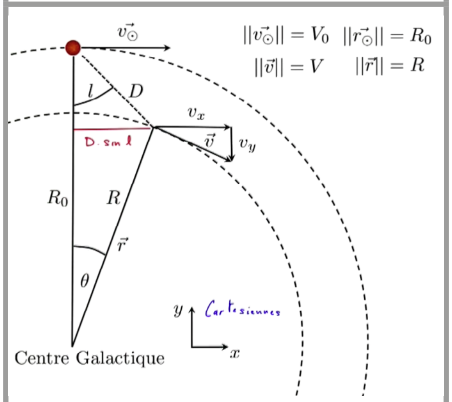

FIGURE 3

7:05 18:59

Cartesian coordinates.

The Milky Way is a Bc spiral galaxy, i.e. a barred spiral galaxy. The total mass of its stars, gas, dust, and dark matter, is $1.2\times10^{12}\ M_\odot$. There are approximately 3×10^{11} stars in the Milky Way. Estimates of its diameter vary between 31 and 37 kpc. The Sun is located 8.3 kpc from the centre of the galaxy.

To describe locations within the Milky Way, we use coordinates defined with respect to the Sun's frame of reference in the Milky Way. The *galactic latitude b* is the angle between the plane of the galaxy and the direction of observation viewed from the side. The *galactic longitude* is the angle between the plane of the galaxy and the direction of observation viewed from the front. We can describe the velocity $\boldsymbol{v}$ of other stars in the galaxy with respect to these coordinates. The relative velocity between the Sun and other stars can be measured and this allows us to study the motion of the Sun within the Milky Way.

Assuming that the Milky Way rotates rigidly, or in other words that all stars have the same angular velocity, then $\omega(\boldsymbol{r}) = \omega_0 = \text{constante}$, where ω_0 is the angular velocity of the Sun.

Consider a Cartesian coordinate system in which the distance and the speed can be decomposed as follows

$$\boldsymbol{v} = R\begin{bmatrix}\cos\theta \\ -\sin\theta\end{bmatrix}\begin{bmatrix}\hat{\boldsymbol{x}} \\ \hat{\boldsymbol{y}}\end{bmatrix}$$

$$\boldsymbol{r} = R\begin{bmatrix}\sin\theta \\ \cos\theta\end{bmatrix}\begin{bmatrix}\hat{\boldsymbol{x}} \\ \hat{\boldsymbol{y}}\end{bmatrix}$$

$$= \begin{bmatrix}D\sin l \\ R_0 - D\cos l\end{bmatrix}\begin{bmatrix}\hat{\boldsymbol{x}} \\ \hat{\boldsymbol{y}}\end{bmatrix} \Rightarrow$$

$$\sin\theta = \frac{D}{R}\sin l, \quad \cos\theta = \frac{R_0}{R} - \frac{D}{R}\cos l$$

This last step eliminates the angle θ, replacing it with $\boldsymbol{l}$, since the latter is the observable quantity. However, we will need different coordinates to describe the radial and tangential velocity of a star with respect to the celestial background. The radial velocity along a line of sight can be measured using the Doppler effect.

In $(\hat{\boldsymbol{x}}, \hat{\boldsymbol{y}})$,

$$v - v_\odot = \begin{bmatrix}V\cos\theta - V_0 \\ -V\sin\theta\end{bmatrix}\begin{bmatrix}\hat{\boldsymbol{x}} \\ \hat{\boldsymbol{y}}\end{bmatrix}, \quad V_0 = \omega_0 R_0, \quad V = \omega R$$

after replacing θ as above

$$v - v_\odot = \begin{bmatrix}R_0(\omega - \omega_0) - \omega D\cos l \\ -D\omega\sin l\end{bmatrix}\begin{bmatrix}\hat{\boldsymbol{x}} \\ \hat{\boldsymbol{y}}\end{bmatrix}$$

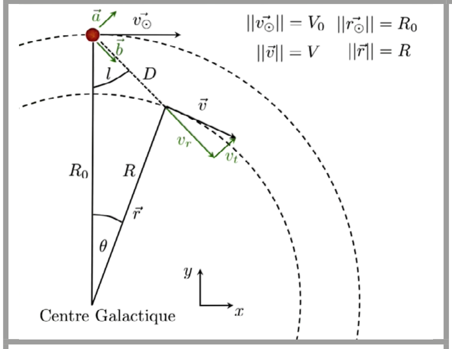

FIGURE 4

8:20 18:59

Polar coordinates a, b.

In this way we can calculate $v - v_\odot$ in the coordinate system $(\hat{x}, \hat{y})$ to project it onto the coordinate system $(\hat{a}, \hat{b})$.

We find that

$$V_r = (\omega - \omega_0) R_0 \sin l \, \hat{b}$$
$$V_t = \left[(\omega - \omega_0) R \cos l - \omega D\right] \hat{a}$$

These equations give us expressions for the radial and tangential velocity of stars relative to the Sun in a coordinate system that is of interest to us, $(\hat{a}, \hat{b})$.

THE SOLAR NEIGHBOURHOOD

In the neighbourhood of the Sun, we have

$$\omega - \omega_0 \approx \left.\frac{d\omega}{dR}\right|_{R_0} (R - R_0)$$

a first-order series expansion of about R_0. From the above equation $V_r = (\omega - \omega_0) R_0 \sin l$, we have

$$V_r = (R - R_0) \left.\frac{d\omega}{dR}\right|_{R_0} R_0 \sin l, \quad \omega = \frac{V}{R}$$
$$\frac{d\omega}{dR} = \frac{\frac{dV}{dR} R - V}{R^2}$$
$$R_0 \left.\frac{d\omega}{dR}\right|_{R_0} = \left[\left.\frac{dV}{dR}\right|_{R_0} - \frac{V_0}{R_0}\right] \quad \text{so}$$
$$V_r = \left[\left.\frac{dV}{dR}\right|_{R_0} - \frac{V_0}{R_0}\right] \sin l \quad \text{and}$$
$$V_t = \left[\left.\frac{dV}{dR}\right|_{R_0} - \frac{V_0}{R_0}\right] (R - R_0) \cos l - \omega D$$

and, since $R - R_0 \approx D \cos L$, we deduce that

$$V_r = AD \sin(2l)$$
$$V_t = AD \cos(2l) + BD \quad \text{where } A \text{ and } B \text{ are the Oort constants}$$
$$A = -\frac{1}{2}\left[\left.\frac{dV}{dR}\right|_{R_0} - \frac{V_0}{R_0}\right]$$
$$B = -\frac{1}{2}\left[\left.\frac{dV}{dR}\right|_{R_0} + \frac{V_0}{R_0}\right]$$

So, assuming that the rotation is rigid

$$V = \omega R \quad \text{with} \quad \omega = \text{constant}$$
$$\frac{dV}{dR} = \omega$$
$$\left.\frac{dV}{dR}\right|_{R_0} = \frac{V_0}{R_0}$$
$$A = 0$$
$$B = \frac{V_0}{R_0}$$

In other words, if A is non-zero, then the rotation must be non-rigid, since depends on R. Measuring these values give

$$\begin{aligned} A &= 14.8 \text{ km}\cdot\text{s}^{-1}\cdot\text{kpc}^{-1} \\ B &= -12.4 \text{ km}\cdot\text{s}^{-1}\cdot\text{kpc}^{-1} \\ A - B &= \frac{V_0}{R_0} = \omega_0 \quad \text{the angular velocity of the Sun within the Milky Way} \\ -(A+B) &= \left.\frac{dV_0}{dR_0}\right|_{R_0} \end{aligned}$$

6.4 DARK MATTER IN GALAXIES AND CLUSTERS OF GALAXIES

Since dark matter does not emit light at any wavelength, two methods have historically been used to detect it: the study of the dynamics of spiral galaxies, and the study of the dynamics of galaxy clusters.

UNIT OF MEASUREMENT

We begin by considering a ratio: the mass of an object in units of solar mass divided by the luminosity of this object in units of solar luminosity. For the Sun,

$$\begin{aligned}\frac{M_\odot}{L_\odot} &= 1 \\ &= 5{,}133 \ \text{kg} \cdot \text{W}^{-1}\end{aligned}$$

This means that if the ratio M/L of an object is larger than that of the Sun, it might contain dark matter, i.e. matter that radiates less than the matter in the Sun.

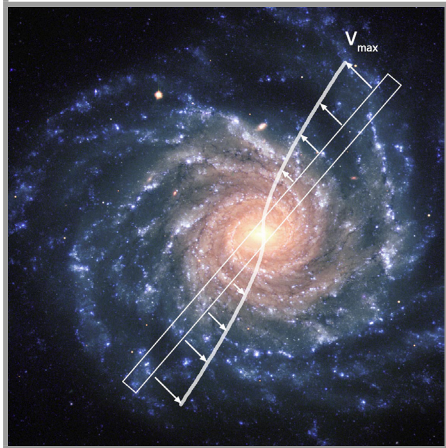

FIGURE 1

3:03 19:44

Spiral galaxy NGC 1232 (image: ESO).

DARK MATTER IN SPIRAL GALAXIES

To reveal the existence of dark matter in spiral galaxies, we can use spectroscopy to measure the velocity vector at different radii across the gap. This gives a *rotation curve* for the galaxy, which shows the radial velocity $v(r)$ as a function of the radius. If the galaxy is tilted at a given angle i relative to the celestial plane, the maximum speed V_{max} satisfies the following relationship with the observed velocity

$$v_{observed} = v_{actual} \sin i$$

In fact, it is necessary to choose a galaxy that is inclined relative to the celestial plane when measuring the rotation speed, since the radial component of the velocity along the line of sight must be known to determine the value of the Doppler effect.

We can, in theory, predict the rotational velocity of the galaxy resulting from the mass within a given radius r

$$\begin{aligned}\frac{GM(r)}{r^2} &= \frac{v^2}{r} \quad \Rightarrow \\ v &= \sqrt{\frac{GM(r)}{r}} \quad \text{(the rotative curve)}\end{aligned}$$

We can then observe how well the velocities near the edge of the galaxy agree with this curve as calculated from the centre of the galaxy. At the centre of the galaxy,

$$\begin{aligned}M(r) &= \frac{4}{3}\pi r^3 \rho \quad \Rightarrow \\ v &= \sqrt{\frac{4G\pi\rho}{3}} r \qquad v \propto r\end{aligned}$$

However, far away from the centre of the galaxy, M is no longer a function of r and

$$v = \sqrt{\frac{GM}{r}} \qquad v \propto \frac{1}{\sqrt{r}}$$

Therefore, these equations predict that the velocity will increase up to the maximum radius of the galaxy, after which it will decrease. However, in practice, we observe that the speed remains constant. There is more mass than is observed at larger radii. To reveal the existence of this mass, we can reverse the equation

$$M(r) = \frac{v^2 r}{G}$$

Since we observe that v is essentially constant at large radii, this predicts that

$$\begin{aligned} \frac{dM(r)}{dr} &= \frac{v^2}{G} \\ &= 4\pi r^2 \rho(r) \quad \Rightarrow \\ \rho(r) &= \frac{v^2}{4\pi G r^2} \quad \Rightarrow \quad \rho \propto \frac{1}{r^2} \end{aligned}$$

However, we observe that

$$\rho \propto \frac{1}{r^{3.5}}$$

The two curves depicting the decrease in density as a function of the radius show that the predicted density decreases more slowly (like $1/r^2$) than the density derived from the luminosity (which decreases like $1/r^{3.5}$).

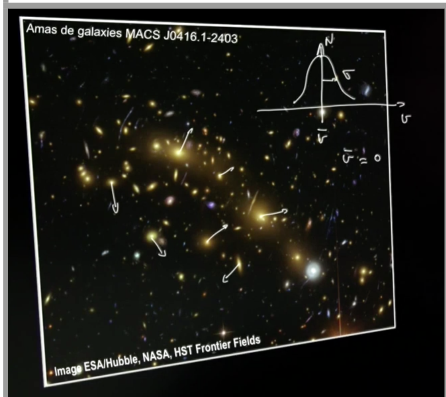

FIGURE 2

12:29 19:44

Galaxy cluster MACS J0416.1-2403 (image: ESA/Hubble, NASA, HST Frontier Fields).

DARK MATTER IN GALAXY CLUSTERS

Galaxy clusters present quite a different situation: there are no longer stars rotating within a disc, but instead large numbers of galaxies, each rotating with their own velocity. All of these galaxies move randomly in every direction. Instead of a rotation curve, the velocity follows an approximately normal distribution with an average velocity close to zero. The spread of these velocities is measured by

$$\sigma^2 = \overline{v^2} - \overline{v}^2 = \overline{v^2}$$

When we use the Doppler effect to measure the velocity of these galaxies, we are measuring the radial velocity rather than the total velocity. We can therefore decompose the velocity into three spherical coordinates $(\hat{r}, \hat{\theta}\ \hat{\rho})$. Since the motion is random:

$$\begin{aligned} \overline{v^2} &= \overline{v_r^2} + \overline{v_\theta^2} + \overline{v_\rho^2} \\ &= 3\overline{v_r^2} = \sigma_r^2 \end{aligned}$$

which describes the spread of the radial velocities.

The virial theorem gives the relationship between the spread of the radial velocities and the mass. Let us say that N galaxies each have mass m giving a total mass of $M=Nm$. According to the virial theorem,

$$-2\langle K \rangle = \langle U \rangle$$

$$-2 \cdot \frac{1}{2}\sum_{i=1}^{N} m_i v_i^2 = -\frac{3}{5}\frac{GM^2}{R} \quad \text{fot the potential energy of a sphere}$$

$$\frac{1}{N}\sum_{i=1}^{N} v_i^2 = \frac{3}{5}\frac{GM}{R} \quad \text{note that the first term is equal to } \overline{v^2}\text{, so}$$

$$\overline{v^2} = 3\overline{v_r^2} = 3\sigma_r^2 = \frac{3}{5}\frac{GM}{R} \quad \Rightarrow$$

$$M = \frac{5R}{G}\sigma_r^2$$

This gives the total mass predicted by the distribution of the observed velocity. In other words, this mass includes everything that is affected by gravity, i.e. both dark matter and luminous matter. We can now measure the luminous mass and compare it with the total mass. And we indeed observe that the luminous mass is lower. In fact, for galaxy clusters, we find that the mass/stellar luminosity ratio is $M/L \approx 100 M_\odot/L_\odot$ whereas for spiral galaxies, the ratio is $M/L = 2 - 10 M_\odot/L_\odot$.

7.1 INTRODUCTION TO COSMOLOGY

Currently, the Big Bang theory is the theory that best explains all of the observations we have been able to make. The Big Bang theory states that the universe was born from a primordial explosion some 13.8 billion years ago, and underwent extremely rapid expansion, followed by a slower rate of expansion. Since the 2000s, we have known that this expansion is accelerating, but we are still completely incapable of explaining why. It can only be explained by invoking the existence of a repulsive force due to an unknown form of energy, known as dark energy that counteracts the gravitational force, which would cause the universe to contract.

HUBBLE'S LAW

The fact that the universe is expanding does not mean that the universe was born at a single point and is expanding like a spherical ball. Instead, it means that every point is moving away from every other by a certain factor, called the *scale factor a*. This makes it possible for two object to remain at the same distance from each other as the universe expands. This *comoving distance* defines the distance between two astronomical bodies in terms of the scale factor. The distance $r(t)$ from an arbitrary point *x* is given by

$$
\begin{aligned}
r(t) &= a(t)x \quad \Rightarrow \quad x = \frac{r(t)}{a(t)} \\
\dot{r}(t) &= \dot{a}(t)x \\
v(r,t) &= \frac{\dot{a}(t)}{a(t)} r(t), \quad \frac{\dot{a}(t)}{a(t)} = H(t) \quad \text{the rate of expansion} \\
v(r_0,t_0) &= H(t_0)r(t_0) \quad \text{and therefore, today} \\
V &= H_0 D \quad \text{Hubble's Law (1929)}
\end{aligned}
$$

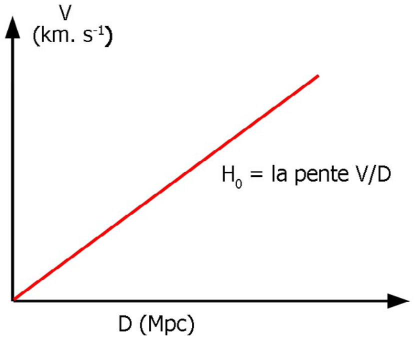

FIGURE 1

5:54 25:53

The Hubble constant.

THE HUBBLE CONSTANT

The Hubble constant:

$$H_0 \approx 70\ \mathrm{km \cdot s^{-1} \cdot Mpc^{-1}}$$

Since kilometres and megaparsecs are both units of distance, the actual scale of H_0 is one over time s^{-1} and $1/H_0$ is the age of the universe, 13.8×10^9 in years.

COSMOLOGICAL REDSHIFT

The Doppler effect can be described by $d\lambda/\lambda$

$$\begin{aligned}
\frac{d\lambda}{\lambda} &= \frac{dv}{c} \\
&= \frac{H(t)dr}{c} \\
&= \frac{\dot{a}}{a}\frac{dr}{c} \\
&= \frac{da}{dt}\frac{dt}{a} = \frac{da}{a} \quad \Rightarrow \\
\lambda &= \frac{d\lambda}{da}a = ka \quad \text{for some constant } k
\end{aligned}$$

Today, $a = 1$, so the emitted λ is equal to the observed λ. The constant k is also equal to this value. We can rewrite these terms as

$$\begin{aligned}
\frac{\lambda_{obs}}{\lambda_{em}} &= \frac{1}{a} \\
\frac{\lambda_{obs} - \lambda_{em}}{\lambda_{em}} &= z \quad \text{the redshift} \quad \Rightarrow \\
\frac{\lambda_{obs}}{\lambda_{em}} &= 1 + z
\end{aligned}$$

So to find the redshift of an object, we measure a particular observed wavelength. Consider the example of a line in a spectrum: if we know its wavelength at rest, i.e. its intrinsic emission wavelength, we can find the redshift: z. This is the well-known formula describing the cosmological Doppler effect.

There are several reasons why the stars have a reddish colour. Some have a lot of dust that has a reddening effect. Others have old, low-mass stellar populations with reddish colours. Finally, there is also a contribution from the cosmological redshift due to the expansion of the universe.

CRITICAL DENSITY

To determine whether or not the universe is a gravitationally bound system, we can write out the balance of kinetic energy and potential energy.

$$\frac{v^2}{2} - \frac{GM}{R} = 0$$

where M is the mass of the universe, R is its typical radius and v is the velocity of a test particle in the universe. Then

$$\begin{aligned}
v &= H_0 R \quad \Rightarrow \\
(H_0 R)^2 &= \frac{2GM}{R} = \frac{2G}{R}\rho\frac{4}{3}\pi R^3 \quad \text{in the case of a spherical universe. Hence} \\
\rho &= \frac{3}{8}\frac{H_0^2}{G\pi} \quad \text{is the critical density of the universe}
\end{aligned}$$

Therefore, if the density of the universe ρ is greater than the critical value ρ, the potential energy is greater than the kinetic energy, we will have contraction, or the expansion will stop. But if ρ is smaller than the critical value ρ, the expansion will be infinite.

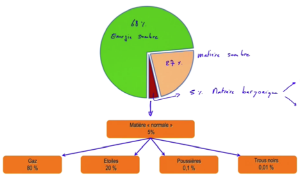

FIGURE 2

17:18 25:53

Composition of the universe.

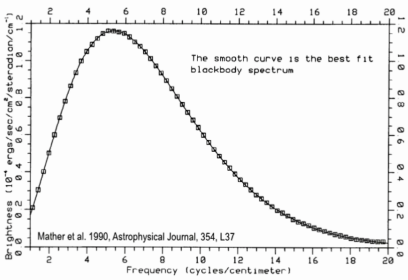

FIGURE 3

17:23 25:53

Cosmic background radiation averaged over the entire sky.

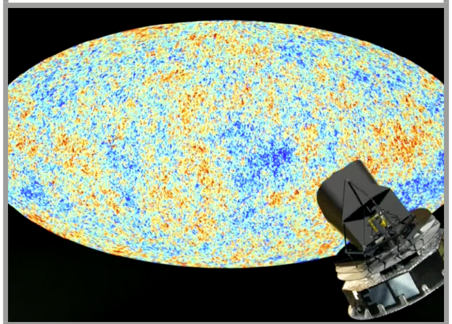

FIGURE 4

22:09 25:53

Map of the universe taken by the satellite Planck 65 (image: ESA Planck Collaboration-D Ducros.).

MAP OF THE UNIVERSE

Currently, within the framework of the Big Bang model, the simple fact that the expansion of the universe is speeding up implies that 68% of the universe consists of dark matter. This dark energy is repulsive, and this explains the accelerated expansion. However, today we believe that only 27% of the universe is dark matter, which suggests that the universe is actually contracting.

5% of all the energy in the universe is in the form of normal matter, known as *baryonic matter*. This matter consists of protons and neutrons together with their electrons. Radiation is emitted by baryonic matter, making it visible. Some of this matter does not emit light, or does not emit light at visible wavelengths. Black holes belong to this category. This invisible portion of normal matter is called “dark matter”. It does not emit any kind of light, at any wavelength.

These figures were derived from observations of the background radiation, which peaks at 2,728°K. This black-body radiation is the same everywhere, except for small spatial variations in the temperature of about 10^{-5}. In 2013-2014, the Planck satellite captured a detailed picture of this background radiation. By subtracting the Milky Way, we obtain an image of the universe when it was 380,000 years old (fig. 4).

At 380,000 years old, the universe was a hot plasma. It was so hot that the protons, photons and electrons were separated in the form of a completely ionized gas. As the universe cooled, as a result of its expansion, the protons in this gas continuously interacted with the electrons until they began to emit photons. These photons immediately propagated in straight lines through a universe that was completely transparent to light, until they reached us. So our map of the universe actually shows what is known as the surface of last scattering. This gives the last time that the photons and electrons were able to interact before the electrons recombined with the protons. This map of the cosmic background radiation is therefore a sort of radiation fossil that shows the imprint of the temperature fluctuations and therefore the density of the universe as it was only 380,000 years after the Big Bang.

7.2 DISTANCE SCALE

There are two methods for measuring distances: one is based on so-called standard metres, whereas the other is based on the standard candles method. The principle of the standard metre approach is to measure how the angular size of an object varies as a function of redshift. Moreover, if we know the physical size of a standard object, we know its distance. We can follow the same reasoning when measuring the apparent luminosity of an object whose intrinsic luminosity, i.e. absolute magnitude, is known. These standard metres and standard candles allow us to link *redshift* to the distance in order to carry out cosmological measurements.

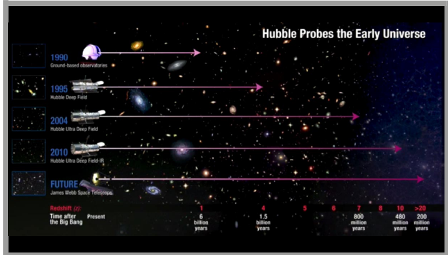

FIGURE 1

2:01 29:22

Redshift and distance.

REDSHIFT AND DISTANCE

As telescopes become increasingly sensitive, we must bear in mind that seeing further away is equivalent to seeing further into the past. This implies that objects will be seen with more and more redshift. The 2010 IR Hubble Deep Field was equipped with an infrared detector in order to see these increasingly redshifted objects.

DISTANCE SCALE

The distance scale can be derived from the fundamental equation

$$1 + z = \frac{1}{\alpha(t)} = \frac{\lambda_{obs}}{\lambda_{em}}$$

where α is the scale factor. The distance from an object is ultimately a function of the redshift/scale factor and the *cosmological parameters*. These cosmological parameters are essentially H_0, but the densities of the various components of the universe, including repulsive dark energy, also play a role.

ANGULAR DIAMETER DISTANCE

If we know the intrinsic radius of an object, we can define a *standard metre* to find the value known as its *angular diameter distance* $D_A(z)$. The angle that subtends the diameter of the object is denoted by ω

$$\omega = \frac{\pi R^2}{D^2}$$

$$D_A(z) = \sqrt{\frac{\pi R^2}{\omega}}$$

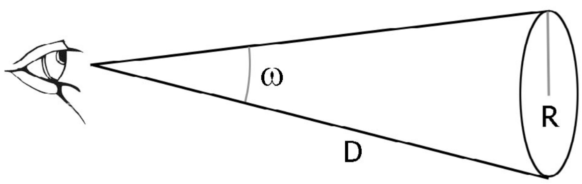

FIGURE 2

5:57 29:22

Definition of the "angle diameter" distance.

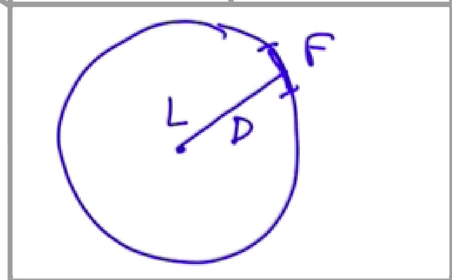

FIGURE 3

7:26 29:22

Definition of the "luminosity distance".

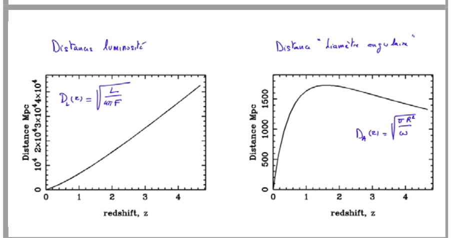

FIGURE 4

9:24 29:22

Luminosity distance and angular diameter distance. (graphs: Refregier *et al.* (2011, Astronomy & Astrophysics, 528, 33) and www.icosmo.org).

LUMINOSITY DISTANCE

Standard candles are defined as stars with a certain known, well-calibrated, well-determined luminosity, which is known as its standard luminosity. If we measure the flux emitted by an object with known intrinsic luminosity, we can infer its distance, which is known as the *luminosity distance*, which depends on *z* (the redshift) measured by the Doppler effect.

$$F = \frac{L}{4\pi D^2}$$

$$D_L(z) = \sqrt{\frac{L}{4\pi F}}$$

In figure 3, we see that the relationship between the redshift and each of the two distances is different. In fact, $D_L(z) = (1+z)^2 D_A(z)$. The angular diameter distance is somewhat counter-intuitive. When considering the luminosity distance, objects become weaker as the *redshift* increases. However, when considering the angular distance diameter, as the *redshift* increases, the angular diameter distance reaches a peak value and then decreases once again. Therefore, objects placed further away tend to appear larger, whereas their brightness continues to decrease.

STANDARD CANDLES

The distance and the speed are combined using Hubble's law

$$V = H_0 D, \quad D = f(z, \text{paramètres cosmologiques})$$

To determine the distance, we use the *distance modulus* μ, where $\mu = m - M = 5\log D_{pc} - 5$ with *m* the apparent magnitude and m the absolute magnitude. If *M* is known (for a standard candle) and *m* is measured, we can calculate the distance. Cepheid stars and supernovae are both used as standard candles.

CEPHEID STARS

Cepheid stars are extremely bright, pulsating supergiants. As their radius varies, their temperature and luminosity also vary, satisfying $L = 4\pi R^2 \sigma T^4$. Therefore, there is a relationship between the frequency and brightness of these Cepheid stars. Luckily, there is a relation between their average absolute magnitude and their period, and the luminosity is proportional to the period.

$$\begin{aligned} \bar{M} &= f(P), \quad L \propto P \\ \bar{M}_V &= -2.43(\log P - 1) - 4.05 \quad \text{in the green filter} \quad \Rightarrow \\ m - \bar{M}_V &= 5\log D_{pc} - 5 \end{aligned}$$

We can use precisely this method with the Hubble Space Telescope to measure the distance of galaxies up to 40-50 Mpc. Some well-known stars are Cepheid stars, including, of course, the star δ Cepheus, which is the archetype of all Cepheid stars. Polaris is also a Cepheid.

TYPE-1A SUPERNOVAE

There are two types to consider. Type-1 supernovae stars are actually a white dwarf and a giant star orbiting around a common centre of gravity. Matter is siphoned away from the giant star to the white dwarf and accumulates around it. After a certain point, the mass reaches a critical threshold ($M_c = 1.44 M_\odot$ the Chandrasekhar limit) which results in a supernova explosion. Since the mass at the time of explosion is always the same, these types of supernova have the same luminosity peak, corresponding to an absolute magnitude of –19.3 in the V band. This absolute magnitude is used (together with the apparent magnitude) in the distance modulus to determine the distance from the supernova.

Supernovae are more useful than Cepheid stars for measuring distances because they are visible from further away. The two characteristics of type 1a supernovae are that the spectrum does not contain a hydrogen line, but instead there are silicon II lines (Singly Ionized Silicon), at a wavelength of 6,150 **Å**. Therefore, when the supernova explodes, we do two things: we take a spectrum to see whether hydrogen and silicon are present, and we measure the light curve to find its apparent magnitude. The distance can then be calculated using the absolute magnitude of –19.3 and the distance modulus.

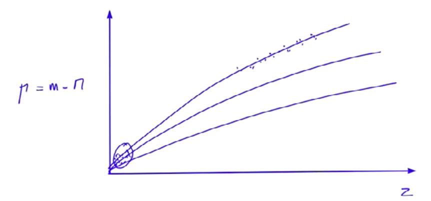

FIGURE 5

9:24 29:22

Hubble diagram: distance modulus vs supernovae *redshift*.

HUBBLE DIAGRAM

The Hubble diagram shows the relationship of the distance modulus to the redshift. These are not observational measurements or predictions, simply a qualitative description. However, it is useful to estimate the cosmological parameters that are most consistent with observations. Most of these parameters relate to the densities of the various components of the universe. It turns out that the densities most consistent with observation are 70% for dark energy, 25% for dark matter, and 5% for baryonic matter.

CONSTRUCTING THE DISTANCE SCALE

To construct the distance scale, we need to attempt to use one measurement method to prove that the others are correct. In our neighbourhood, we can use the parallaxes within the Milky Way up to distances of approx. 40-50 Mpc. Beyond the Milky Way, we can use Cepheid stars, and further still, we can use type-1a supernovae. There are therefore several intercalibration regions where we can compare the results of one method with another. In the vicinity of the Milk Way, both Cepheid stars and the parallax method can be used to estimate the distance. Further away, there is a region in which we must rely primarily on Cepheid stars, but there are occasionally supernovae that can be used for comparison. They are relatively uncommon, since each galaxy has roughly one type-1a supernovae per century. We currently know of around a dozen. Further away still, beyond 40-50 Mpc, supernovae are the only available indicators of distance.

7.3 GRAVITATIONAL LENSING

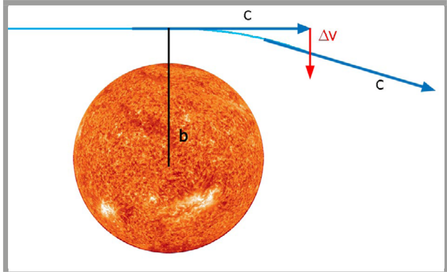

FIGURE 1

3:07 33:28

Deflection angle of the light caused by mass (in this example, the Sun).

Gravitational lensing is a phenomenon also known as *gravitational mirages*. Light is deflected not because of a change in the refractive index of the propagation medium, as in the desert, but as a result of a strong gravitational field such as that created by a galaxy, a star, or a galaxy cluster. The light from a distance star is bent as it passes by massive objects in the foreground, causing the star's image to become distorted. By studying this distortion, we can calculate the mass of the object in the foreground, whether or not it is visible. The deflection angle is denoted by $\hat{\alpha}$. Thus

$$\hat{\alpha} = \frac{|\Delta v|}{|c|}$$

$\hat{\alpha}$ is very small, in the order of a few tenths of an arcsecond at most.

$$\Delta v = \frac{GM}{b^2}\Delta t, \quad \Delta t \approx \frac{b}{c} \quad \text{order of magnitude} \Rightarrow$$
$$\hat{\alpha} \approx \frac{GM}{c^2 b}$$

We can see that the angle of deflection $\hat{\alpha}$ only depends on the mass of the lens and the impact parameter. $\hat{\alpha}$ does not depend on the wavelength. In practice, Newton's theory and Einstein's theory predict different values of $\hat{\alpha}$.

$$\hat{\alpha}(Newton) = \frac{2GM}{c^2 b}$$
$$\hat{\alpha}(Einstein) = \frac{4GM}{c^2 b}$$

By taking measurements during a solar eclipse, we can find the relationship between the deflection caused by the mass and the radius of the Sun.

$$\hat{\alpha} = 1.75'' \left(\frac{M}{M_\odot}\right)\left(\frac{b}{R_\odot}\right)$$

The value of 1.75" is consistent with the predictions made by general relativity.

The fundamental difference between $\hat{\alpha}$ (Newton) and $\hat{\alpha}$ (Einstein) lies in the fact that in the Newtonian framework of gravity, photons follow curved paths in Euclidean space, whereas in the framework of general relativity photons follow straight paths in curved space. These paths are known as geodesics, and represent the shortest path between two points in curved space.

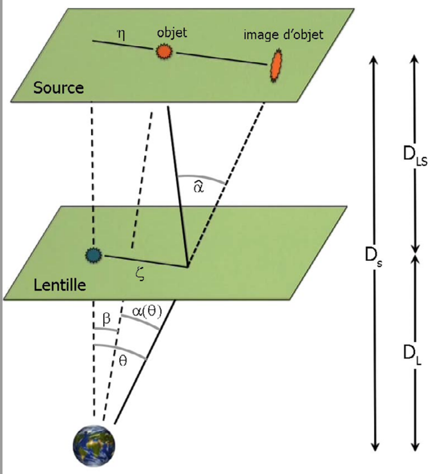

FIGURE 2

13:18 33:28

Gravitational lensing phenomenon.

LENS EQUATION

With the angles and distances defined in figure 2, we can find the angle of deflection of the image of the object itself, $\alpha(\theta)$, from the point of view of the observer. We can rewrite the lens equation in terms of the angles

$$\beta = \theta - \alpha(\theta) \quad \text{ou}$$

$$\eta = \frac{D_S}{D_L}\zeta - D_{LS}\hat{\alpha}(\zeta) \quad \Rightarrow$$

$$\alpha(\theta) = \frac{D_{LS}}{D_S}\hat{\alpha}(\zeta)$$

in terms of linear distances.

THE EINSTEIN RADIUS

The Einstein radius is an extremely important characteristic quantity. If the source, the lens, and the observer are aligned, then

$$\theta = \frac{D_{LS}}{D_S}\cdot\frac{4GM}{c^2\zeta}$$

$$= \frac{D_{LS}}{D_S}\cdot\frac{4GM}{c^2\theta D_L} \quad \Rightarrow$$

$$\theta_E = \sqrt{\frac{D_{LS}}{D_S}\cdot\frac{4GM}{c^2 D_L}} \quad \text{(the Einstein radius)}$$

Thus, when everything is aligned ($\beta = 0$), the lens equation has infinitely many solution distributed over a ring of diameter $2\theta_E$ and the source image takes the form of a ring around the lens galaxy.

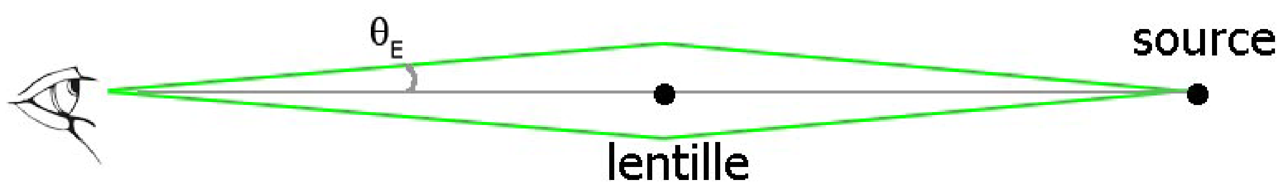

FIGURE 3

15:46 33:28

The Einstein radius.

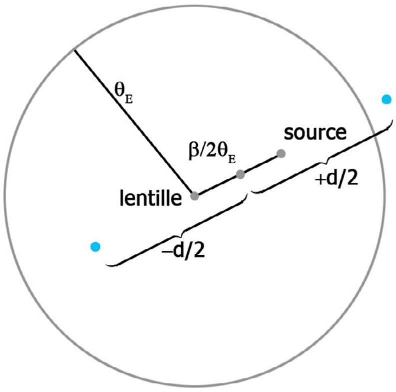

FIGURE 4

20:40 33:28

Case of a single-point lens.

CASE OF A SINGLE-POINT LENS

$$\beta = \theta - \alpha(\theta), \quad \alpha(\theta) = \frac{\theta_E^2}{\theta} \Rightarrow$$
$$= \theta - \frac{\theta_E^2}{\theta} \Rightarrow$$

The equation is therefore quadratic for θ.

$$\theta^2 - \beta\theta - \theta_E^2 = 0 \Rightarrow$$
$$\theta = \frac{1}{2}\left(\beta \pm \sqrt{\beta^2 + 4\theta_E^2}\right)$$
$$\frac{\theta}{\theta_E} = \frac{1}{2}\left(\frac{\beta}{\theta_E} \pm \underbrace{\sqrt{\frac{\beta}{\theta_E^2} + 4}}_{d_\pm}\right)$$

The ± means that, if the lens is a single point, two mirage images will form on either side of the source, separated by a distance d. In the simple case where the lens is represented by a point mass, we can predict that there will be two mirage images of the background object. However, in slightly more realistic models, an odd number of images is predicted, either 3 or 5 depending on the shape of the lens in the foreground.

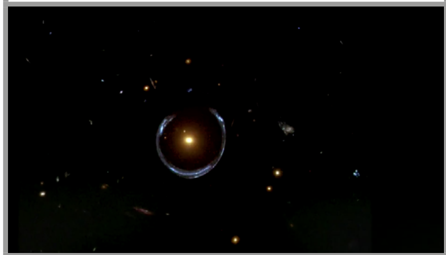

FIGURE 5

22:22 33:28

A perfect Einstein ring
(image: ESA/Hubble-NASA).

APPLICATIONS TO GALAXIES

We can calculate the mass within an Einstein ring as follows

$$\theta_E = \sqrt{\frac{GM}{c^2}\frac{D_{LS}}{D_S D_L}} \Rightarrow M(\theta_E)$$

We can see that the gravitational lens effect is an extremely powerful tool for measuring the mass as a function of the radius. We can measure the total mass, including both luminous and dark matter, by gravitational lensing, since it depends only on gravity. We don't necessarily need to be able to see the mass in order to measure its effect on background objects.

APPLICATIONS TO THE WHOLE UNIVERSE

As well as the strong gravitational lensing effect, which produces multiple images of background objects such as Einstein rings, there is also a weak gravitational lensing effect. All images that reach us from far away (and therefore from the past) are deformed by mass to some extent. The deformation predicted by each cosmological model varies as a function of H_0 and its composition in terms of dark energy and dark matter. Measuring this deformation can be used to test each proposed cosmological model.

IMPRESSUM

Layout:
Emphase Sàrl, Lausanne

Summary: Charles McCall

Developed by the EPFL Press, BOOCs (Books and Open Online Courses) provide the accompanying text for MOOCs at the Swiss Federal Institute of Technology in Lausanne (EPFL).
They create a real learning advantage and bring added value to the MOOC, summarizing the main points to remember to help obtain the qualification.
Learn faster, learn better. Happy studying!

ISBN 978-2-88914-XXX-X